IMPERIAL

Imperial College London

Department of Mathematics

The Generalised Grey Bergomi Model

Author: Adriano Oliveri Orioles (CID: 02384387)

A thesis submitted for the degree of

MSc in Mathematics and Finance, 2023-2024

Declaration

The work contained in this thesis is my own work unless otherwise stated.

Acknowledgements

I would like to thank my academic supervisor Dr. Antoine Jacquier for his time and feedback throughout my thesis. His thought-provoking discussions and insights were instrumental in the completion of this thesis.

I would also like to thank my girlfriend Jamie and my family for their unconditional love and support throughout my studies.

Abstract

In this thesis, a generalisation of the rough Bergomi model is proposed (referred to as the generalised grey Bergomi model) which uses generalised grey Brownian motion, a special class of H-sssi (H-self-similar-stationary-increments) processes that provide non-semimartingale variance stochastic models for anomalous diffusion. For $\beta = 1$, fractional Brownian motion is retrieved [31], thus, giving a fresh starting point for constructing rough volatility models. VIX dynamics under the generalised grey Bergomi model are characterised; alongside this, a numerical scheme is given to price VIX Futures and Options. General pricing schemes are also provided, showcasing the superiority of the generalised grey Bergomi model over the rough Bergomi model in terms of implied volatility curve generation. Most importantly, the discounted stock price process is shown to be a martingale under this new model, which is essential for derivative pricing.

Contents

List of Figures

List of Tables

Introduction

A decade ago, Gatheral, Jaisson, and Rosenbaum made a case for non-semimartingale volatility processes in [24], making the case that volatility is "rough" (linked to the Hölder regularity of the paths from the volatility process). This led to many stochastic volatility models having a "rough" counterpart developed (for example the rough Heston model [18] and rough Bergomi model [5]). These new rough models swapped the standard Brownian motion in place for the fractional counterpart, where the fractional counterpart is defined as the process for which $t \in [0, T]$ has $\mathbb{E}[B_t^H] = 0$ and covariance function

$$\mathbb{E}[B_t^H B_s^H] := \frac{1}{2}\left(t^H + s^H - |t-s|^H\right),$$

with $H \in (0, 1)$ (referred to as the Hurst parameter). For $H = \frac{1}{2}$, one obtains standard Brownian motion. Meanwhile, for $H < \frac{1}{2}$, the increments of the process are negatively correlated, and for $H > \frac{1}{2}$, the increments of the process are positively correlated. In other words, when $H < \frac{1}{2}$, fractional Brownian motion (fBm) has short-term dependencies and when $H > \frac{1}{2}$, fBm has long-term dependencies.

Returning to [24], it was noted that the volatility process observed through market prices had Hurst parameter $H \approx 0.1$. This observation is the fundamental reason for the popularity of rough volatility models such as the ones mentioned above.

Since then, one of the open problems in mathematical finance has been to solve the SPX-VIX joint calibration problem. Due to its importance and difficulty, this problem has even been referred to as "the holy grail of volatility modeling" [25]. Several attempts have been made, with the most promising being the Quadratic Rough Heston (qrHeston) model in [25]. Whilst the qrHeston model is appealing in theory, in practice calibration is much more time consuming since there are six parameters to calibrate (compared to three parameters in the rough Bergomi model).

Coincidentally, several years before [24], Mainardi et al. [31, 32] showed that the marginal density function of the class $\{B_t^{\beta,\alpha}, t \geq 0\}$, referred to as generalised grey Brownian motion (ggBm), is the fundamental solution to the stretched time-fractional diffusion equation. By construction, this class is made up of self-similar processes with stationary increments and Hurst parameter $H = \alpha/2$. Therefore, ggBm is a special class of H-sssi (H-self-similar-stationary-increments) processes that provide non-semimartingale variance stochastic models. For $\beta = 1$, fBm is retrieved [31], thus, giving a fresh starting point for the construction of rough volatility models. This ultimately leads to novel dynamics of the forward variance.

Model-wise, the starting point is the rough Bergomi model, a simple and robust model. However, like any model, the rough Bergomi model is not perfect. This is mainly due to the log-normal forward variance causing VIX smiles to be flat, which, is not consistent with market data. The aim of this thesis is to construct a generalised version of the rough Bergomi model which resolves this issue and potentially solves the SPX-VIX joint calibration problem without introducing too many extra parameters to calibrate.

In light of this, the organisation of this thesis is as follows: Chapter 1 gives a general introduction to ggBm. Chapter 2 follows with the construction of the generalised grey

Bergomi (ggBergomi) model. In Chapter 3 it is proven that, under certain conditions, the discounted stock price process is a martingale. Moreover, Chapter 3 is dedicated to an array of VIX analyses; this includes a discussion of VIX simulation schemes and calibrating the ggBergomi model to VIX Futures. To conclude, Chapter 4 discusses general simulation methods for the ggBergomi model. Additionally, calibration to SPX Options under the ggBergomi model is highlighted.

An important point to mention is that the foundation of this thesis is largely inspired by the unpublished work in [28].

Chapter 1

Generalised Grey Brownian Motion

1.1 Introducing the M-Wright Distribution

For $\beta > 0$, the standard Mittag-Leffler function $\mathcal{E}_\beta$ is defined as an entire function by the series representation

$$\mathcal{E}_\beta(z) := \sum_{n\geq 0} \frac{z^n}{\Gamma(\beta n + 1)}$$

for all $z \in \mathbb{C}$, where Γ denotes the Gamma function. Subsequently, the three-parameter Mittag-Leffler function $\mathcal{E}^\gamma_{\alpha,\beta}$ for any $z \in \mathbb{C}$ is defined as [22]

$$\mathcal{E}^\gamma_{\alpha,\beta}(z) := \frac{1}{\Gamma(\gamma)} \sum_{n\geq 0} \frac{\Gamma(\gamma + n) z^n}{n!\Gamma(\alpha n + \beta)}, \quad \alpha, \beta, \gamma \in \mathbb{C}, \quad \mathrm{Re}(\alpha) > 0. \tag{1.1.1}$$

Finally, the M-Wright function $\mathcal{M}_\beta$ for $\beta \in (0, 1]$ is defined as

$$\mathcal{M}_\beta(z) := \sum_{n\geq 0} \frac{(-z)^n}{n!\Gamma(-\beta n + 1 - \beta)} \quad \text{for } z \in \mathbb{C}. \tag{1.1.2}$$

Note that the choice $\beta = \frac{1}{2}$ reduces the M-Wright function to the Gaussian density. By using Euler's reflection formula $\Gamma(z)\Gamma(1 - z) = \frac{\pi}{\sin(\pi z)}$, with $z = \beta(n + 1)$, one can write

$$\mathcal{M}_\beta(z) = \frac{1}{\pi} \sum_{n\geq 0} \frac{(-z)^n}{n!} \sin\left(\pi\beta(n + 1)\right) \Gamma(\beta(n + 1)).$$

Thus, when $\beta = \frac{1}{2}$,

$$\begin{aligned}
\mathcal{M}_{\frac{1}{2}}(z) &= \frac{1}{\pi} \sum_{n\geq 0} \frac{(-z)^n}{n!} \sin\left(\pi \frac{n+1}{2}\right) \Gamma\left(\frac{n+1}{2}\right) \\
&= \frac{1}{\pi} \sum_{p\geq 0} \frac{(-z)^{2p}}{(2p)!} \sin\left(\pi \frac{2p+1}{2}\right) \Gamma\left(\frac{2p+1}{2}\right) \\
&= \frac{1}{\pi} \sum_{p\geq 0} \frac{(-z)^{2p}}{(2p)!} \sin\left(\pi\left(p + \frac{1}{2}\right)\right) \Gamma\left(p + \frac{1}{2}\right) \\
&= \frac{1}{\pi} \sum_{p\geq 0} \frac{(-z)^{2p}}{(2p)!} (-1)^p \frac{(2p)!}{4^p p!} \sqrt{\pi} \\
&= \frac{1}{\sqrt{\pi}} \sum_{p\geq 0} \frac{1}{p!} \left(-\frac{z^2}{4}\right)^p = \frac{1}{\sqrt{\pi}} \exp\left\{-\frac{z^2}{4}\right\}
\end{aligned}$$

by using the identities $\sin\left(\pi\frac{2p}{2}\right) = 0$, $\Gamma\left(p+\frac{1}{2}\right) = \frac{(2p)!}{4^p p!}\sqrt{\pi}$, and $\sin\left(\pi\left(p+\frac{1}{2}\right)\right) = (-1)^p$. As shown in [31], the Mittag-Leffler function $\mathcal{E}_\beta$ and the M-Wright function are related through the Laplace transform

$$\int_0^\infty \mathrm{e}^{-su}\mathcal{M}_\beta(u)\mathrm{d}u = \mathcal{E}_\beta(-s),$$

valid for any $s \geq 0$.

To conclude, a random variable Y_β follows the (one-sided) M-Wright distribution if it is supported on the positive half line and admits the M-Wright function in Equation (1.1.2) as the probability density function. Furthermore, its moment of order $\kappa > -1$ exists [34] and is given by

$$\mathbb{E}\left[Y_\beta^\kappa\right] = \frac{\Gamma(1+\kappa)}{\Gamma(1+\beta\kappa)}. \tag{1.1.3}$$

Remark 1.1.1. Note that most programming languages do not have a built-in package for M-Wright variate generation (with the sole exception being R [10]). For an introduction to M-Wright variate generation, the reader is referred to Appendix A.

1.2 Defining Generalised Grey Brownian Motion

Definition 1.2.1 (Generalised grey Brownian motion)**.** Let $\beta \in (0,1]$ and $\alpha \in (0,2)$. A generalised grey Brownian motion (ggBm) $B^{\beta,\alpha}$ defined on a complete probability space $(\Omega, \mathcal{F}, \mathbb{P})$ is a one-dimensional continuous stochastic process starting from $B_0^{\beta,\alpha} = 0$, $\mathbb{P}$-almost surely, such that, for any $0 \leq t_1 < t_2 < \ldots < t_n < \infty$, the joint characteristic function is given by

$$\mathbb{E}\left[\exp\left\{\mathrm{i}\sum_{k=1}^n u_k B_{t_k}^{\beta,\alpha}\right\}\right] = \mathcal{E}_\beta\left(-\frac{1}{2}\mathbf{u}^\top\Sigma_\alpha\mathbf{u}\right) \quad \text{for any } \mathbf{u} = (u_1,\ldots,u_n) \in \mathbb{R}^n,$$

where $\Sigma_\alpha := \frac{1}{2}\left(t_k^\alpha + t_j^\alpha - |t_k - t_j|^\alpha\right)_{k,j=1}^n$ denotes the covariance matrix.

Since Σ_α corresponds precisely to the covariance matrix of a fractional Brownian motion with Hurst parameter $\alpha/2$, it is trivially symmetric positive definite.

Remark 1.2.2. As mentioned before, when $\beta = 1$, one retrieves fractional Brownian motion (fBm) [31]. By the same token, taking $\beta = \alpha = 1$ reduces ggBm to the classical Brownian motion. This can be verified quickly by checking the joint characteristic function defined above.

Remark 1.2.3. Note that within a Physics context, the factor $1/2$ is not present in the expression of Σ_α. This is due to the convention of normalising the standard Brownian motion with a variance (at time 1) of 2 as opposed to a normalisation of 1, which is standard practice in probability theory.

By the inverse Fourier transform, the joint characteristic function above is integrable and rapidly decreasing; therefore, the distribution is absolutely continuous and the joint probability density function of $\left(B_{t_1}^{\beta,\alpha},\ldots,B_{t_n}^{\beta,\alpha}\right)$ is equal to [15]

$$f_\beta(\mathbf{u}) = \frac{(2\pi)^{-\frac{n}{2}}}{\sqrt{\det\Sigma_\alpha}}\int_0^\infty\left[\tau^{-\frac{n}{2}}\exp\left\{-\frac{1}{2\tau}\mathbf{u}^\top\Sigma_\alpha^{-1}\mathbf{u}\right\}\right]\mathcal{M}_\beta(\tau)\mathrm{d}\tau.$$

Further computations show that the moments of $B_t^{\beta,\alpha}$ are given by

$$\mathbb{E}\left[\left(B_t^{\beta,\alpha}\right)^{2n+1}\right] = 0 \qquad \text{and} \qquad \mathbb{E}\left[\left(B_t^{\beta,\alpha}\right)^{2n}\right] = \frac{(2n)!}{2^n\Gamma(\beta n+1)}t^{n\alpha}, \quad t \geq 0, n \in \mathbb{N},$$

and its covariance function by

$$\mathbb{E}\left[B_t^{\beta,\alpha}B_s^{\beta,\alpha}\right] = \frac{t^\alpha + s^\alpha - |t-s|^\alpha}{2\Gamma(\beta+1)} \qquad \text{for all } t, s \geq 0.$$

Furthermore, for each $t, s \geq 0$, the characteristic function of the increments reads

$$\mathbb{E}\left[\exp\left\{\mathrm{i}u\left(B_t^{\beta,\alpha} - B_s^{\beta,\alpha}\right)\right\}\right] = \varphi_{t-s}(u) \qquad \text{for all } u \in \mathbb{R}, \tag{1.2.1}$$

where

$$\varphi_\delta(u) := \mathcal{E}_\beta\left(-\frac{u^2}{2}|\delta|^\alpha\right) \quad \text{for any } \delta, u \in \mathbb{R}. \tag{1.2.2}$$

Since the Mittag-Leffler function $\mathcal{E}_\beta$ is not quadratic, it is clear that the marginals of $B^{\beta,\alpha}$ are not Gaussian and Equation (1.2.1) shows that it is $\frac{\alpha}{2}$-self-similar with stationary increments. As shown in [14], the sample paths of $B^{\beta,\alpha}$ have finite p-variation for any $p > \frac{2}{\alpha}$, therefore, implying that it is not a semimartingale whenever $\alpha \in (0,1)$. Similarly, when $\alpha \in (1,2)$, [36] shows that $B^{\beta,\alpha}$ cannot be a semimartingale either. The following is an important property that will be central in the rest of the computations:

Lemma 1.2.4 ([33, Proposition 3])**.** *The generalised grey Brownian motion admits the representation*

$$B_t^{\beta,\alpha} \overset{(d)}{=} \sqrt{Y_\beta}B_t^{\frac{\alpha}{2}},$$

for all $t \geq 0$, where $B^{\frac{\alpha}{2}}$ is a standard fractional Brownian motion with Hurst parameter $\frac{\alpha}{2}$ and Y_β an independent non-negative random variable with density $\mathcal{M}_\beta(\cdot)$.

To conclude this chapter, consider the characteristic function in Equation (1.2.1) and Equation (1.2.2) for $0 < s < t$, and then the following analytic extension can be obtained for all $u \in \mathbb{R}$:

$$\mathfrak{M}_{t-s}(u) := \varphi_{t-s}(-\mathrm{i}u) = \mathbb{E}\left[\mathrm{e}^{u\left(B_t^{\beta,\alpha} - B_s^{\beta,\alpha}\right)}\right] = \mathcal{E}_\beta\left(\frac{u^2}{2}|t-s|^\alpha\right).$$

This is well-defined and positive, thus, it fully characterises a moment-generating function.

Chapter 2

The Generalised Grey Bergomi Model

Consider the rough Bergomi model originally proposed by Bayer et al. [5] with risk-neutral dynamics

$$\begin{aligned} \mathrm{d}X_t &= \left(r - \frac{1}{2}V_t\right)\mathrm{d}t + \sqrt{V_t}\mathrm{d}W_t, \quad X_0 = 0, \\ V_t &= \xi_0(t)\mathcal{E}^{\Diamond}\left(\eta B_t^H\right), \qquad\qquad V_0 > 0, \end{aligned}$$

where $\xi_0(\cdot) > 0$ denotes the forward variance curve, $\eta > 0$ is a volatility of volatility parameter, $r \in \mathbb{R}$ is the risk-free rate, and $H \in (0,1)$ is the Hurst parameter governing the Hölder regularity of the fractional Brownian motion B^H, which is correlated with the standard Brownian motion W with correlation $\rho \in [-1,1]$. Both noise processes are adapted to the same canonical filtration. Here, $\mathcal{E}^{\Diamond}$ denotes the Wick exponential

$$\mathcal{E}^{\Diamond}(Z) \coloneqq \exp\left\{Z - \frac{1}{2}\mathbb{E}\left[|Z|^2\right]\right\},$$

since the Doléans-Dade exponential

$$\mathcal{E}(Z) := \exp\left\{Z - \frac{1}{2}[Z]\right\},$$

where $[\cdot]$ denotes the quadratic variation, is in general not well defined for fractional Brownian motion because the latter is not a semi-martingale for $H \neq \frac{1}{2}$ [36]. The rough Bergomi model exhibits VIX dynamics that closely resemble the log-normal distribution [28]. As a result, under the rough Bergomi model, the VIX smile is almost flat, which is not consistent with upward-sloping smiles in data. Moreover, insofar as the stochastic volatility framework, the volatility-of-volatility parameter is not deterministic [2, 3, 20]. This leads one to the conclusion that a stochastic volatility-of-volatility parameter is needed for solving joint SPX and VIX calibration problems. However, [37] shows that the calibration problem is largely solvable with two-factor volatility models.

Given the aforementioned points, it is natural to introduce a new factor in the form of random volatility-of-volatility parameter $\tilde{\eta} : \Omega \to \mathbb{R}^+$, so that the volatility process in this new rough Bergomi-inspired model is given by

$$V_t = \xi_0(t)\mathcal{E}^{\blacklozenge}\left(\tilde{\eta}B_t^H\right), \quad \xi_0(t) > 0, \quad t \in [0,T],$$

where for any $\eta > 0$ the stochastic exponential is defined as

$$\mathcal{E}^{\blacklozenge}(\eta Z) \coloneqq \exp\left\{\eta Z - \log \mathfrak{M}_{\cdot}^{Z}(\eta)\right\}, \quad \text{for } t \in [0,T],$$

where $\mathfrak{M}^Z$ is the moment-generating function of Z. Thus, whenever well-defined, this ensures $\mathbb{E}\left[\mathcal{E}^{\blacklozenge}(\eta Z)\right] = 1$ and collapses into the standard Wick exponential $\mathcal{E}^{\diamondsuit}(\eta Z)$ in the case where Z is a centred Gaussian process. By definition, the forward variance is defined as $\xi_s(t) := \mathbb{E}[V_t|\mathcal{F}_s]$, for $0 \leq s \leq t$, so that in particular $\xi_0(t) := \mathbb{E}[V_t]$, which explains the requirement $\mathbb{E}\left[\mathcal{E}^{\blacklozenge}(\eta Z)\right] = 1$.

Now choose $\tilde{\eta} = \eta\sqrt{Y_\beta}$ for $\eta > 0$, where Y_β is an independent non-negative random variable with probability density function $\mathcal{M}_\beta(\tau)$ for $\tau \geq 0$. Thus, using Lemma 1.2.4, the model can be viewed as a generalisation of the rough Bergomi model [5] with a random volatility-of-volatility coefficient.

The risk-neutral dynamics of the generalised grey Bergomi (ggBergomi) are therefore given by

$$\begin{aligned} \mathrm{d}X_t &= \left(r - \tfrac{1}{2}V_t\right)\mathrm{d}t + \sqrt{V_t}\left(\rho \mathrm{d}B_t + \sqrt{1-\rho^2}\mathrm{d}W_t\right), \quad X_0 = 0, \\ V_t &= \xi_0(t)\mathcal{E}^{\blacklozenge}\left(\eta B_t^{\beta,\alpha}\right), \qquad\qquad\qquad\qquad\quad V_0 > 0, \end{aligned} \tag{2.0.1}$$

where $\xi_0(\cdot) > 0$ again denotes the forward variance curve, $\eta > 0$, $r \in \mathbb{R}$ is the risk-free rate, and $\rho \in [-1, 1]$ is the correlation parameter between the standard Brownian motions W and B. Here, $B^{\beta,\alpha}$ with $\alpha \in (0, 2)$ and $\beta \in (0, 1]$ is the ggBm from Definition 1.2.1 and is related to the Brownian motion B through the relation in Lemma 1.2.4.

Remark 2.0.1. Note that in theory any random variable can be chosen in place of the one-sided M-Wright random variable Y_β. In this case, Y_β is chosen due to the convenient result in Lemma 1.2.4. Potentially, justification of one's choice in random variable might be found on the VVIX front but this is left for further research.

For any $t > 0$, let $\mathcal{F}_t^Z := \sigma(Z_t)$ be the sigma algebras for $Z \in \{W, B\}$, $\mathcal{F}_t^{\mathscr{B}} := \sigma(B_t^{\beta,\alpha})$, and $\mathcal{F}_t := \mathcal{F}_t^W \vee \mathcal{F}_t^{\mathscr{B}}$. Using Lemma 1.2.4 yields $\mathcal{F}_t^{\mathscr{B}} = \sigma(Y_\beta B_t^{\frac{\alpha}{2}})$ and, furthermore, by Lemma B.0.1 we have that $\mathcal{F}_t^{\mathscr{B}} = \sigma(Y_\beta) \vee \mathcal{F}_t^B$. Finally, the filtrations generated by W and $B^{\beta,\alpha}$ are denoted by $\mathbb{F}^W$ and $\mathbb{F}^{\mathscr{B}}$m respectively, and $\mathbb{F} := \mathbb{F}^W \vee \mathbb{F}^{\mathscr{B}}$.

To use this model in the absence of arbitrage opportunities, the discounted stock price process $(S_t)_{t\geq 0} := (\exp\{X_t - rt\})_{t\geq 0}$ must be an $\mathbb{F}$-martingale. It is shown in Chapter 3 that this is indeed the case.

Chapter 3

VIX in the Generalised Grey Bergomi Model

Expanding the stochastic exponential in the variance process from Equation (2.0.1), one can write

$$\begin{aligned} V_t &= \xi_0(t)\mathcal{E}^{\blacklozenge}(\eta B_t^{\beta,\alpha}) = \xi_0(t)\exp\left\{\eta B_t^{\beta,\alpha} - \log\mathcal{E}_\beta\left(\frac{\eta^2}{2}t^\alpha\right)\right\} \\ &= \xi_0(t)\mathcal{E}_\beta\left(\frac{\eta^2 t^\alpha}{2}\right)^{-1}\exp\left\{\eta B_t^{\beta,\alpha}\right\}, \end{aligned}$$

so that the VIX squared can be expressed as

$$\begin{aligned} \mathrm{VIX}_T^2 &= \frac{1}{\Delta}\int_T^{T+\Delta}\mathbb{E}\left[V_s|\mathcal{F}_T^{\mathscr{B}}\right]ds = \frac{1}{\Delta}\int_T^{T+\Delta}\xi_0(s)\mathcal{E}_\beta\left(\frac{\eta^2 s^\alpha}{2}\right)^{-1}\mathbb{E}\left[\mathrm{e}^{\eta B_s^{\beta,\alpha}}\middle|\mathcal{F}_T^{\mathscr{B}}\right]ds \\ &= \frac{1}{\Delta}\int_T^{T+\Delta}\xi_0(s)\mathcal{E}_\beta\left(\frac{\eta^2 s^\alpha}{2}\right)^{-1}\mathbb{E}\left[\exp\left\{\eta\sqrt{Y_\beta}B_s^{\alpha/2}\right\}\middle|\mathcal{F}_T^{B},Y_\beta\right]ds. \end{aligned}$$

As opposed to the rough Bergomi model where the VIX process is close to log-normal, the VIX process here is not close to log-normal as long as $\beta \neq 1$.

Note that the conditional expectation $\mathbb{E}\left[\exp\left(\eta\sqrt{Y_\beta}B_s^{\alpha/2}\right)\middle|\mathcal{F}_T^{\mathscr{B}}\right]$ is difficult to evaluate; to circumvent this, one can redefine ggBm using Riemann-Liouville fBm.

3.1 Generalised Grey Riemann-Liouville Brownian Motion

For an introduction to necessary concepts such as nuclear spaces and Minlos' Theorem, the reader is encouraged to first read Appendix C. From [16] it is known that standard fBm has the spectral representation

$$B_t^{\frac{\alpha}{2}} = \sqrt{C(\alpha)}\int_{\mathbb{R}}\frac{1}{\sqrt{\pi}}\frac{e^{itx}-1}{ix}|x|^{\frac{1-\alpha}{2}}d\widetilde{B}_x, \quad t\geq 0,$$

$$C(\alpha) := \Gamma(\alpha+1)\sin\frac{\pi\alpha}{2},$$

where (with a slight abuse of notation) $d\widetilde{B}(x) = dB_1(x)+idB_2(x)$ with $dB_1(x) = dB_1(-x)$ and $dB_2(x) = -dB_2(-x)$. Moreover, B_1 and B_2 are independent Brownian motions. Notice that

$$\frac{1}{\sqrt{\pi}}\frac{e^{itx}-1}{ix} = \tilde{1}_{[0,t)}(x),$$

where $\tilde{f}$ is the Fourier transform of the function f. Thus, standard fBm can be written as

$$B_t^{\frac{\alpha}{2}} = \sqrt{C(\alpha)} \int_{\mathbb{R}} \tilde{1}_{[0,t)}(x)|x|^{\frac{1-\alpha}{2}} d\widetilde{B}_x, \quad t \geq 0.$$

The choice in defining standard fBm in this way will become apparent, but with the last point one can define a generalised stochastic process X such that for a suitable test function ϕ one has

$$X_\alpha(\phi) = \sqrt{C(\alpha)} \int_{\mathbb{R}} \widetilde{\phi}(x)|x|^{\frac{1-\alpha}{2}} d\widetilde{B}_x.$$

As in [32], consider the space of test functions to be

$$\{f \in \mathcal{L}^2(\mathbb{R}) \mid ||f||_\alpha^2 = C(\alpha) \int_{\mathbb{R}} |\widetilde{f}(x)|^2 |x|^{1-\alpha} dx < \infty\}. \tag{3.1.1}$$

Thus, $B_t^{\frac{\alpha}{2}} = X_\alpha\left(1_{[0,t)}\right)$ and

$$\mathbb{E}\left[\left(B_t^{\frac{\alpha}{2}}\right)^2\right] = ||1_{[0,t)}||_\alpha^2 = t^\alpha,$$

and auto-covariance

$$\mathbb{E}\left[B_t^{\frac{\alpha}{2}} B_s^{\frac{\alpha}{2}}\right] = \frac{1}{2}(t^\alpha + s^\alpha - |t-s|^\alpha).$$

Now consider the Schwarz space $\mathcal{S}(\mathbb{R})$ instead of $\mathcal{L}^2(\mathbb{R})$, and equip it with the scalar product

$$(f,g)_\alpha = C(\alpha) \int_{\mathbb{R}} \overline{\widetilde{f}(x)} \widetilde{g}(x)|x|^{1-\alpha} dx, \quad f,g \in \mathcal{S}(\mathbb{R}), \quad 0 < \alpha < 2.$$

Notice that the scalar product above generates the α-norm in (3.1.1). Let $\mathcal{S}_0^{(\alpha)}(\mathbb{R})$ denote the completion of $\mathcal{S}(\mathbb{R})$ with respect to (3.1.1). From [32] it is known that $\mathcal{S}(\mathbb{R})$ is a nuclear space with respect to the topology generated by the α-norm and an operator $A^{(\alpha)}$.

By Proposition C.0.4, with the choice of $F_\beta(t) = \mathcal{E}_\beta(-t)$, for $t \geq 0$, $0 < \beta \leq 1$, the functional $\Phi_{\alpha,\beta}(\xi) = F_\beta(||\xi||_\alpha^2)$ defines a characteristic function on $\mathcal{S}(\mathbb{R})$. Furthermore, by Minlos' Theorem, one can guarantee the existence of a unique probability measure $\mu_{\alpha,\beta}$ defined on $(\mathcal{S}'(\mathbb{R}), \mathcal{B})$ such that

$$\int_{\mathcal{S}'(\mathbb{R})} e^{i\langle\omega,\xi\rangle} d\mu_{\alpha,\beta}(\omega) = \mathcal{E}_\beta\left(\frac{1}{2}||\xi||_\alpha^2\right), \quad \xi \in \mathcal{S}(\mathbb{R}),$$

where $\langle\cdot,\cdot\rangle$ is the natural bilinear pairing between $\mathcal{S}(\mathbb{R})$ and $\mathcal{S}'(\mathbb{R})$, and $\mathcal{S}'(\mathbb{R})$ is the dual of $\mathcal{S}(\mathbb{R})$ which is equipped with the weak topology.

Definition 3.1.1 (Definition 3.1 [32])**.** The generalised stochastic process $X_{\alpha,\beta}$ defined canonically on the "generalised" grey noise space $(\mathcal{S}'(\mathbb{R}), \mathcal{B}, \mu_{\alpha,\beta})$ is called "generalised" grey noise. Therefore, for each test function $\xi \in \mathcal{S}(\mathbb{R})$,

$$X_{\alpha,\beta}(\xi)(\cdot) = \langle\cdot,\xi\rangle.$$

By construction the generalised stochastic process $X_{\alpha,\beta}$ in Definition 3.1.1 has the characteristic function

$$\mathbb{E}[e^{i\eta X_{\alpha,\beta}(\xi)}] = \mathcal{E}_\beta\left(-\frac{1}{2}\eta^2||\xi||_\alpha^2\right).$$

With this, the notion of generalised grey Riemann-Liouville Brownian motion can be defined.

Definition 3.1.2 (Generalised Grey Riemann-Liouville Brownian Motion)**.** Let $\beta \in (0,1]$, $\alpha \in (0,2)$. Generalised grey Riemann-Liouville Brownian motion (ggRLBm) $B_{\mathrm{RL}}^{\beta,\alpha}$ defined on $(\mathcal{S}'(\mathbb{R}), \mathcal{B}, \mu_{\alpha,\beta})$ is defined as

$$B_{\mathrm{RL},t}^{\beta,\alpha} := X_{\alpha,\beta}\left(\frac{C_{\frac{\alpha}{2}} 1_{[0,t)}}{\sqrt{\alpha}}\right),$$

where $C_{\frac{\alpha}{2}} := \frac{1}{\Gamma(\frac{1}{2}(1+\alpha))}$.

Furthermore, similarly to ggBm, ggRLBm has the following properties:

1. $B_{\mathrm{RL},0}^{\beta,\alpha} = 0$ a.s.;
2. for each $t \geq 0$, the moments are

$$\mathbb{E}\left[B_{\mathrm{RL},t}^{\beta,\alpha}\right] = 0 \quad \text{and} \quad \mathbb{E}\left[\left(B_{\mathrm{RL},t}^{\beta,\alpha}\right)^2\right] = \frac{C_{\frac{\alpha}{2}}^2}{\alpha\Gamma(\beta+1)} t^\alpha;$$

3. the auto-covariance function is

$$\mathbb{E}\left[B_{\mathrm{RL},t}^{\beta,\alpha} B_{\mathrm{RL},s}^{\beta,\alpha}\right] = \frac{C_{\frac{\alpha}{2}}^2}{2\alpha\Gamma(\beta+1)}(t^\alpha + s^\alpha - |t-s|^\alpha);$$

4. for any $t, s \geq 0$, the characteristic function is

$$\mathbb{E}\left[e^{iu(B_{\mathrm{RL},t}^{\beta,\alpha} - B_{\mathrm{RL},s}^{\beta,\alpha})}\right] = \mathcal{E}_\beta\left(-\frac{u^2 C_{\frac{\alpha}{2}}^2 |t-s|^\alpha}{2\alpha}\right), \quad u \in \mathbb{R}. \tag{3.1.2}$$

Remark 3.1.3. All the properties of ggBm trivially carry over since ϕ is simply being scaled. Thus, by [32, Proposition 3.2], for $0 < \alpha < 1$ and $\beta \in (0,1]$ with $t \geq 0$, the process $B_{\mathrm{RL},t}^{\beta,\alpha}$ is self-similar with stationary increments where $H = \alpha/2$. Note that the subtle change of using Riemann-Lioville fBm instead of standard fBm in Lemma 1.2.4 implies that ggRLBm is not the same process as ggBm. Instead, by Definition 3.1.1, ggRLBm is a separate "generalised" grey noise.

Remark 3.1.4. As before, by considering the characteristic function in Equation (3.1.2) for $0 < s < t$ and by analytically extending the characteristic function, one has that for all $u \in \mathbb{R}$,

$$\mathfrak{M}_{t-s}(u) \coloneqq \varphi_{t-s}(-\mathrm{i}u) = \mathbb{E}\left[\mathrm{e}^{u\left(B_{\mathrm{RL},t}^{\beta,\alpha} - B_{\mathrm{RL},s}^{\beta,\alpha}\right)}\right] = \mathcal{E}_\beta\left(\frac{u^2 C_{\frac{\alpha}{2}}^2 |t-s|^\alpha}{2\alpha}\right).$$

This is well-defined and positive, thus, it fully characterises a moment-generating function.

Remark 3.1.5. Lemma 1.2.4 yields the decomposition

$$B_{\mathrm{RL},t}^{\beta,\alpha} \overset{(d)}{=} \sqrt{Y_\beta} C_{\frac{\alpha}{2}} \int_0^t (t-s)^{\frac{1}{2}(\alpha-1)} dB_s.$$

As mentioned in Chapter 2, to use this model in the absence of arbitrage opportunities, the discounted stock price process $(S_t)_{t\geq 0}$ must be an $\mathbb{F}$-martingale. The following theorem summarises when this is the case:

Theorem 3.1.6. *Let K be a kernel such that*

$$\int_0^t K(t,s)dB_s$$

defines a Gaussian process (conditional on a one-sided M-Wright random variable Y_β) with continuous sample paths, $\sigma : [0,\infty)\times\mathbb{R} \to \mathbb{R}_+$ is continuous and bounded on $[0,T]\times(-\infty,a]$ for each T, $a > 0$. If $\rho \leq 0$, then $(S_t)_{t\geq 0}$ defined by the generalised grey Bergomi model is a true martingale.

A proof of this (building on [23]) is given in Appendix B.

Remark 3.1.7. One could potentially use the ggBm process directly in the ggBergomi model by using the integral representation from [7, Theorem 6]

$$B_t^{\beta,\alpha} \overset{(d)}{=} \frac{\cos\frac{\alpha\pi}{2}}{\pi}\int_0^\infty \sqrt{Y_\beta}X_x(t)\frac{dx}{x^{\frac{1}{2}(\alpha+1)}},$$

where $X_x(t)$ is an Ornstein-Uhlenbeck process with respect to a Brownian motion B. However, with this integral representation of ggBm, VIX dynamics become considerably more convoluted to derive and, as such, are left for further study.

3.1.1 VIX Dynamics

Using ggRLBm in the ggBergomi model results in the VIX dynamics from Proposition 3.1.8. Note that the analysis conducted here uses the same ideas as in [27].

Proposition 3.1.8. *The VIX dynamics using ggRLBm are given by*

$$\Delta\,\mathrm{VIX}_T^2 = \int_T^{T+\Delta}\xi_0(s)\mathcal{E}_\beta\left(\frac{\eta^2 C_{\frac{\alpha}{2}}^2 s^\alpha}{2\alpha}\right)^{-1}\zeta_T(s)\exp\left\{\eta^2 Y_\beta C_{\frac{\alpha}{2}}^2\frac{(s-T)^\alpha}{2\alpha}\right\}ds.$$

where $\zeta_T(s) := \exp\left\{\eta\sqrt{Y_\beta}C_{\frac{\alpha}{2}}\mathcal{V}_s^T\right\}$.

Proof. Let $\mathcal{V}_t := \int_0^t (t-u)^{\frac{1}{2}(\alpha-1)}dB_u$. By previous arguments,

$$\begin{aligned}\Delta\,\mathrm{VIX}_T^2 &= \int_T^{T+\Delta}\xi_0(s)\mathcal{E}_\beta\left(\frac{\eta^2 C_{\frac{\alpha}{2}}^2 s^\alpha}{2\alpha}\right)^{-1}\mathbb{E}\left[\exp\left\{\eta\sqrt{Y_\beta}C_{\frac{\alpha}{2}}\mathcal{V}_s\right\}\middle|\mathcal{F}_T^B, Y_\beta\right]ds\\ &= \int_T^{T+\Delta}\xi_0(s)\mathcal{E}_\beta\left(\frac{\eta^2 C_{\frac{\alpha}{2}}^2 s^\alpha}{2\alpha}\right)^{-1}\mathbb{E}\left[\exp\left\{\eta\sqrt{Y_\beta}C_{\frac{\alpha}{2}}(\mathcal{V}_{s,T}+\mathcal{V}_s^T)\right\}\middle|\mathcal{F}_T^B, Y_\beta\right]ds,\end{aligned}$$

where

$$\mathcal{V}_{t,T} := \int_T^t (t-u)^{\frac{1}{2}(\alpha-1)}dB_u \quad \text{and} \quad \mathcal{V}_t^T := \int_0^T (t-u)^{\frac{1}{2}(\alpha-1)}dB_u.$$

Now define the random variable $\zeta_T(s) := \exp\left\{\eta\sqrt{Y_\beta}C_{\frac{\alpha}{2}}\mathcal{V}_s^T\right\}$. Since $\zeta_T(s) \in \mathcal{F}_T^{\mathscr{B}}$, one has that

$$\Delta\,\mathrm{VIX}_T^2 = \int_T^{T+\Delta}\xi_0(s)\mathcal{E}_\beta\left(\frac{\eta^2 C_{\frac{\alpha}{2}}^2 s^\alpha}{2\alpha}\right)^{-1}\zeta_T(s)\mathbb{E}\left[\exp\left\{\eta\sqrt{Y_\beta}C_{\frac{\alpha}{2}}\mathcal{V}_{s,T}\right\}\middle|\mathcal{F}_T^B, Y_\beta\right]ds.$$

Moreover, $\mathcal{V}_{s,T}$ is a centered Gaussian process with variance

$$\mathbb{V}\mathrm{ar}(\mathcal{V}_{s,T}) = \frac{(s-T)^\alpha}{\alpha},$$

which is independent of $\mathcal{F}_T^B$. Thus,

$$\mathbb{E}\left[\exp\left\{\eta\sqrt{Y_\beta}\mathcal{V}_{s,T}\right\}\middle|\mathcal{F}_T^B,\sigma(Y_\beta)\right]=\exp\left\{\eta^2 Y_\beta C_{\frac{\alpha}{2}}^2\frac{(s-T)^\alpha}{2\alpha}\right\}.$$

Therefore,

$$\Delta\,\mathrm{VIX}_T^2=\int_T^{T+\Delta}\xi_0(s)\mathcal{E}_\beta\left(\frac{\eta^2C_{\frac{\alpha}{2}}^2\,s^\alpha}{2\alpha}\right)^{-1}\zeta_T(s)\exp\left\{\eta^2Y_\beta C_{\frac{\alpha}{2}}^2\frac{(s-T)^\alpha}{2\alpha}\right\}ds.$$

□

3.2 VIX Futures in the Generalised Grey Bergomi Model

The risk-neutral formula for a VIX future $\mathfrak{B}_T$ with maturity T is given by

$$\begin{aligned}\mathfrak{B}_T:=\mathbb{E}\left[\mathrm{VIX}_T\,|\mathcal{F}_0^B\right]&=\mathbb{E}\left[\sqrt{\frac{1}{\Delta}\int_T^{T+\Delta}\mathbb{E}\left[\mathrm{d}\langle X_s,X_s\rangle|\mathcal{F}_T^{\mathscr{B}}\right]}\middle|\mathcal{F}_0^B\right]\\&=\mathbb{E}\left[\sqrt{\frac{1}{\Delta}\int_T^{T+\Delta}\xi_T(s)ds}\middle|\mathcal{F}_0^B\right].\end{aligned}\tag{3.2.1}$$

Proposition 3.2.1. *Using Definition 3.1.2, the forward variance curve ξ_T in the ggBergomi model admits the representation*

$$\xi_T(t)=\xi_0(t)\mathcal{E}_\beta\left(\frac{\eta^2C_{\frac{\alpha}{2}}^2\,t^\alpha}{2\alpha}\right)^{-1}\zeta_T(t)\exp\left\{\eta^2Y_\beta C_{\frac{\alpha}{2}}^2\frac{(t-T)^\alpha}{2\alpha}\right\},\quad\textit{for any } t\geq T.$$

Proof. Since $\mathbb{E}[V_t|\mathcal{F}_t^{\mathscr{B}}]=\xi_T(t)$ by Equation (3.2.1), the result follows from Proposition 3.1.8 and the equality

$$\mathbb{E}[V_t|\mathcal{F}_t^{\mathscr{B}}]=\xi_0(t)\mathcal{E}_\beta\left(\frac{\eta^2C_{\frac{\alpha}{2}}^2\,t^\alpha}{2\alpha}\right)^{-1}\zeta_T(t)\exp\left\{\eta^2Y_\beta C_{\frac{\alpha}{2}}^2\frac{(t-T)^\alpha}{2\alpha}\right\}.$$

□

3.2.1 Upper and lower bounds for VIX Futures

Using Definition 3.1.2, one can construct upper and lower bounds for VIX Futures.

Proposition 3.2.2. *The following bounds hold for VIX Futures:*

$$\begin{aligned}\frac{1}{\Delta}\int_T^{T+\Delta}\sqrt{\xi_0(s)}\mathcal{E}_\beta\left(\frac{\eta^2C_{\frac{\alpha}{2}}^2\,s^\alpha}{2}\right)^{-\frac{1}{2}}\mathcal{E}_\beta\left(\frac{\eta^2C_{\frac{\alpha}{2}}^2\left[s^\alpha+(s-T)^\alpha\right]}{8\alpha}\right)ds&\\\leq\mathfrak{B}_T\leq\sqrt{\frac{1}{\Delta}\int_T^{T+\Delta}\xi_0(s)ds}.&\end{aligned}$$

Proof. The conditional Jensen's inequality and Fubini's theorem (since ξ_T is $\mathcal{F}_0^B$-adapted) give

$$\mathfrak{B}_T=\mathbb{E}[\mathrm{VIX}_T\,|\mathcal{F}_0]=\mathbb{E}\left[\sqrt{\frac{1}{\Delta}\int_T^{T+\Delta}\xi_T(s)ds}\middle|\mathcal{F}_0\right]\leq\sqrt{\frac{1}{\Delta}\int_T^{T+\Delta}\mathbb{E}[\xi_T(s)|\mathcal{F}_0]ds}.$$

Then by the martingale property of ξ_T,

$$\mathfrak{B}_T \leq \sqrt{\frac{1}{\Delta}\int_T^{T+\Delta} \xi_0(s)ds}.$$

For the lower bound, Proposition 3.2.1 and the Cauchy-Schwarz inequality yield

$$\begin{aligned}
\mathfrak{B}_T &= \mathbb{E}\left[\mathrm{VIX}_T \middle| \mathcal{F}_0^B\right] \\
&= \mathbb{E}\left[\sqrt{\frac{1}{\Delta}\int_T^{T+\Delta} \xi_0(s)\mathcal{E}_\beta\left(\frac{\eta^2 C_{\frac{\alpha}{2}}^2 s^\alpha}{2\alpha}\right)^{-1} \zeta_T(s)\exp\left\{\eta^2 Y_\beta C_{\frac{\alpha}{2}}^2 \frac{(s-T)^\alpha}{2\alpha}\right\} ds}\middle| \mathcal{F}_0^B\right] \\
&\geq \mathbb{E}\left[\frac{1}{\Delta}\int_T^{T+\Delta} \sqrt{\xi_0(s)\mathcal{E}_\beta\left(\frac{\eta^2 C_{\frac{\alpha}{2}}^2 s^\alpha}{2\alpha}\right)^{-1} \zeta_T(s)\exp\left\{\eta^2 Y_\beta C_{\frac{\alpha}{2}}^2 \frac{(s-T)^\alpha}{4\alpha}\right\} ds}\middle| \mathcal{F}_0^B\right].
\end{aligned}$$

Furthermore, by Fubini's theorem

$$\begin{aligned}
\mathfrak{B}_T &\geq \frac{1}{\Delta}\int_T^{T+\Delta} \sqrt{\xi_0(s)}\mathcal{E}_\beta\left(\frac{\eta^2 C_{\frac{\alpha}{2}}^2 s^\alpha}{2\alpha}\right)^{-\frac{1}{2}} \mathbb{E}\left[\sqrt{\zeta_T(s)}\exp\left\{\eta^2 Y_\beta C_{\frac{\alpha}{2}}^2 \frac{(s-T)^\alpha}{4\alpha}\right\}\middle| \mathcal{F}_0^B\right] ds \\
&= \frac{1}{\Delta}\int_T^{T+\Delta} \sqrt{\xi_0(s)}\mathcal{E}_\beta\left(\frac{\eta^2 C_{\frac{\alpha}{2}}^2 s^\alpha}{2\alpha}\right)^{-\frac{1}{2}} \mathbb{E}\left[\mathbb{E}\left[\sqrt{\zeta_T(s)}\exp\left\{\eta^2 Y_\beta C_{\frac{\alpha}{2}}^2 \frac{(s-T)^\alpha}{4\alpha}\right\}\middle| Y_\beta\right]\middle| \mathcal{F}_0^B\right] ds \\
&= \frac{1}{\Delta}\int_T^{T+\Delta} \sqrt{\xi_0(s)}\mathcal{E}_\beta\left(\frac{\eta^2 C_{\frac{\alpha}{2}}^2 s^\alpha}{2\alpha}\right)^{-\frac{1}{2}} \mathbb{E}\left[\exp\left\{\eta^2 Y_\beta C_{\frac{\alpha}{2}}^2 \left(\frac{s^\alpha + (s-T)^\alpha}{8\alpha}\right)\right\}\middle| \mathcal{F}_0^B\right] ds \\
&= \frac{1}{\Delta}\int_T^{T+\Delta} \sqrt{\xi_0(s)}\mathcal{E}_\beta\left(\frac{\eta^2 C_{\frac{\alpha}{2}}^2 s^\alpha}{2\alpha}\right)^{-\frac{1}{2}} \sum_{n=0}^{\infty}\frac{1}{n!}\left(\frac{\eta^2 C_{\frac{\alpha}{2}}^2 \left[s^\alpha + (s-T)^\alpha\right]}{8\alpha}\right)^n \mathbb{E}\left[Y_\beta^n\right] ds \\
&= \frac{1}{\Delta}\int_T^{T+\Delta} \sqrt{\xi_0(s)}\mathcal{E}_\beta\left(\frac{\eta^2 C_{\frac{\alpha}{2}}^2 s^\alpha}{2\alpha}\right)^{-\frac{1}{2}} \mathcal{E}_{\beta,1}^1\left(\frac{\eta^2 C_{\frac{\alpha}{2}}^2 \left[s^\alpha + (s-T)^\alpha\right]}{8\alpha}\right) ds \\
&= \frac{1}{\Delta}\int_T^{T+\Delta} \sqrt{\xi_0(s)}\mathcal{E}_\beta\left(\frac{\eta^2 C_{\frac{\alpha}{2}}^2 s^\alpha}{2\alpha}\right)^{-\frac{1}{2}} \mathcal{E}_\beta\left(\frac{\eta^2 C_{\frac{\alpha}{2}}^2 \left[s^\alpha + (s-T)^\alpha\right]}{8\alpha}\right) ds,
\end{aligned}$$

where in the third equality $\sqrt{\zeta_T(s)}$ is log-normal (conditional on Y_β) with mean

$$\exp\left\{\eta^2 Y_\beta C_{\frac{\alpha}{2}}^2 \frac{s^\alpha - (s-T)^\alpha}{8\alpha}\right\},$$

in the third last equality the moments of Y_β are defined in Equation (1.1.3), and in the second last equality the three-parameter Mittag-Lefler function from Equation (1.1.1) is used. □

To gain some intuition as to how tight these bounds are in comparison to a Monte Carlo estimate of VIX Futures, consider the parameters

$$\alpha = 0.14, \quad \beta = 0.5, \quad \eta = 1.2287,$$

with the following three scenarios from [27] for the initial forward variance curve:

- Scenario 1: $\xi_0(t) = 0.235^2$;
- Scenario 2: $\xi_0(t) = 0.235^2(1+t)^2$;
- Scenario 3: $\xi_0(t) = 0.235^2\sqrt{1+t}$.

Figure 3.1 showcases the upper and lower bounds for the three scenarios described above.

Remark 3.2.3. Figure 3.1 suggests that the bounds in Proposition 3.2.2 are not tight, except for when $\beta = 1$ (when the ggBergomi model collapses to the rough Bergomi model) [27]. This can be attributed to the added variance of the random variable Y_β.

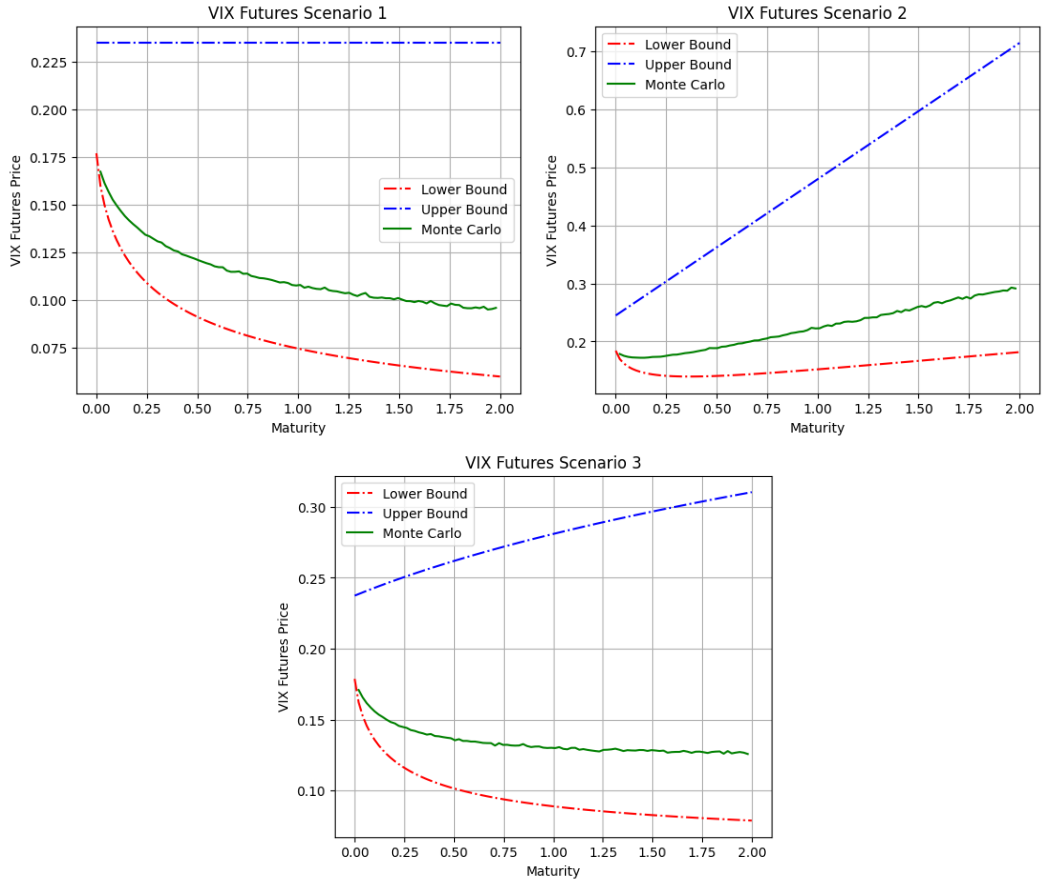

Figure 3.1: Upper and lower bounds in all three scenarios.

3.3 Numerical Implementation of the VIX Process

In this section, a truncated Cholesky decomposition simulation scheme is presented for the VIX in the ggBergomi model. This scheme is identical to the one found in [27], the only difference being the forward variance structure. For analysis of the computational complexity of the scheme, the reader is referred directly to [27].

The covariance structure of $\mathcal{V}^T$ on $[T, T+\Delta]$ is given by

$$\begin{aligned}\mathbb{E}[\mathcal{V}_t^T \mathcal{V}_s^T] &= \int_0^T [(t-u)(s-u)]^{\frac{1}{2}(\alpha-1)} du \qquad (3.3.1)\\ &= \frac{(s-t)^{\frac{1}{2}(\alpha-1)}}{\frac{1}{2}(\alpha+1)} \left\{ t^{\frac{1}{2}(\alpha+1)} F\left(\frac{-t}{s-t}\right) - (t-T)^{\frac{1}{2}(\alpha+1)} F\left(\frac{T-t}{s-t}\right) \right\},\end{aligned}$$

for any $t < s$, where

$$F(u) := {}_2F_1\left(-\frac{1}{2}(\alpha+1), \frac{1}{2}(\alpha+1), 1+\frac{1}{2}(\alpha+1), u\right),$$

and ${}_2F_1$ is the hypergeomtric function [1, Chapter 15].

In this scheme the dependence structure is modelled exactly on the first 8 points due to the same numerical reasons as in [27] and the remaining points are calculated by correlating and rescaling using Equation (3.3.1). The scheme can be summarised as follows:

Algorithm 3.3.1 (VIX simulation (truncated Cholesky))**.** Fix a grid $\mathfrak{T} = \{\tau_j\}_{j=0,\dots,N}$ on $[T, T+\Delta]$,

1. compute the covariance matrix of $(\mathcal{V}^T_{\tau_i})_{i=1,\dots,8}$ using Equation (3.3.1);

2. generate $\{\mathcal{V}^T_{\tau_j}\}_{j=1,\dots,N}$ by correlating and rescaling using Equation (3.3.1):

$$\mathcal{V}^T_{\tau_j} = \sqrt{\mathbb{V}[\mathcal{V}^T_{\tau_j}]}\left(\frac{\rho(\mathcal{V}^T_{\tau_{j-1}}, \mathcal{V}^T_{\tau_j})\mathcal{V}^T_{\tau_{j-1}}}{\sqrt{\mathbb{V}[\mathcal{V}^T_{\tau_{j-1}}]}} + \sqrt{1-\rho(\mathcal{V}^T_{\tau_{j-1}}, \mathcal{V}^T_{\tau_j})^2}\mathcal{N}(0,1)\right), \quad \text{for } j = 9, \dots, N;$$

3. compute the VIX via numerical integration, for example using a composite trapezoidal rule:

$$\text{VIX}_T \approx \sqrt{\frac{1}{\Delta}\sum_{j=0}^{N-1}\frac{Q^2_{T,\tau_j} + Q^2_{T,\tau_{j+1}}}{2}(\tau_j - \tau_{j-1})},$$

where $Q^2_{T,\tau_j} := \xi_0(\tau_j)\mathcal{E}_\beta\left(\frac{\eta^2 C^2_{\frac{\alpha}{2}}\tau_j^\alpha}{2}\right)^{-1}\exp\left\{\eta\sqrt{Y_\beta}C_{\frac{\alpha}{2}}\widetilde{\mathcal{V}}^T_{\tau_j}\right\}\exp\left\{\eta^2 Y_\beta C^2_{\frac{\alpha}{2}}\frac{(\tau_j - T)^\alpha}{2\alpha}\right\}.$

Numerical experiment

As before, using the same parameters used in [5, 6], one has that

$$\xi_0(t) = 0.235^2, \quad \alpha = 0.14, \quad \beta = 0.5, \quad \eta = 1.2287.$$

Figure 3.2 shows the results for 10^5 Monte Carlo Simulations for the Truncated Cholesky scheme. As a comparison, VIX Futures prices and Monte Carlo standard deviations as a function of maturity for the rough Bergomi (denoted by rBergomi in the legend) are also given. Meanwhile, only results for the Monte Carlo standard deviation as a function of the number of simulations and the computational time in the ggBergomi model are given.

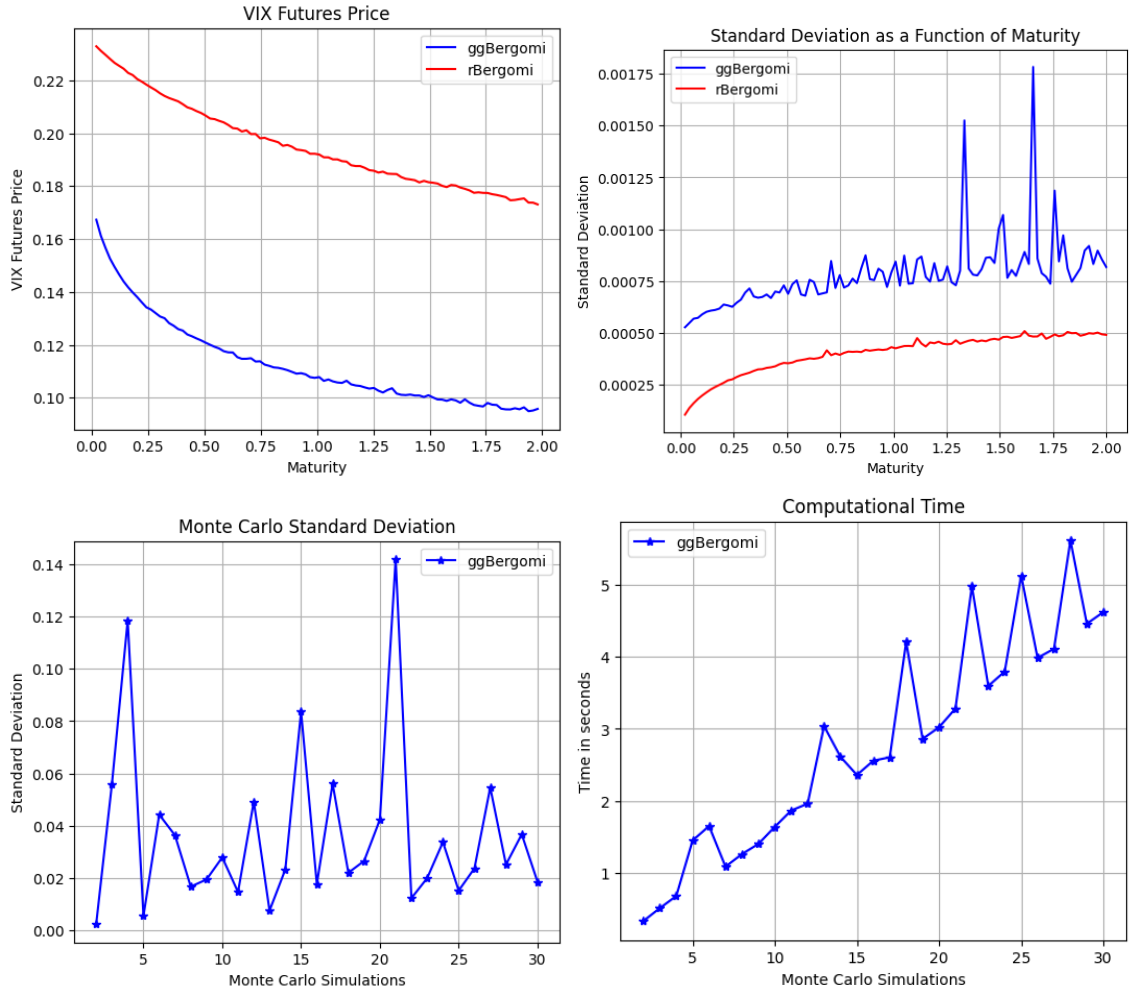

Figure 3.2: Truncated Cholesky Monte Carlo results.

Remark 3.3.2. In comparison to the rough Bergomi model results from [27] (where $\beta = 1$), the Monte Carlo results (where $\beta = 0.5$) have a considerably higher standard deviation. The reason for this is that as β increases, the variance of the random variable decreases. An example of this can be seen in Figure A.1. To compensate for this, a higher number of Monte Carlo simulations are required in the ggBergomi.

Remark 3.3.3. The introduction of the random variable Y_β causes the jumps observed in the computational time and Monte Carlo standard deviation plots in Figure 3.2. On the standard deviation front, extreme values of Y_β will skew the Monte Carlo estimate and, consequently, the Monte Carlo standard deviation.

3.4 VIX Futures Calibration in the Generalised Grey Bergomi Model

Objective function

To calibrate the ggBergomi model to VIX Futures, define the objective function

$$\mathcal{L}^{\mathfrak{F}}(\alpha) := \sum_{i=1}^{N} (\mathfrak{B}_{T_i} - \mathfrak{F}_i)^2,$$

which is minimised over (α, β, η). Note that $(\mathfrak{F}_i)_{i=1,\dots,N}$ are the observed Futures prices [1] at times $T_1 < \ldots < T_N$ and $\mathfrak{B}_{T_i}$ are the Futures prices obtained in the ggBergomi model.

Remark 3.4.1. Unlike in [5, 27], the forward variance in the ggBergomi model is not log-normal (unless $\beta = 1$). Thus one cannot take advantage of pricing formulae by assuming that the VIX payoff is log-normal as in the rough Bergomi model. This means that VIX Futures calibration in the ggBergomi model takes orders of magnitude longer than in the rough Bergomi model. For this reason, alongside time constraints, VIX Futures calibration in the ggBergomi model has been omitted and is reserved for future study.

Obtaining the initial forward variance curve

For large maturities, analysing the limiting behaviour of ξ_0 is of interest. It is known that ξ_0 can be decomposed using the total implied variance via the relation

$$\xi_0(t) = \frac{\mathrm{d}}{\mathrm{d}t} t\sigma_0^2(t) = \sigma_0^2(t) + t\frac{\mathrm{d}}{\mathrm{d}t}\sigma_0^2(t).$$

Thus, it suffices to understand limiting behaviour of $t\sigma_0^2(t)$ (the total implied variance). Due to the abundance of high-quality data, a cubic Hermite spline is fitted on total variance space [2].

Remark 3.4.2. Note that using a cubic Hermite spline is only feasible when the data has high fidelity. If there are large jumps between adjacent points, then the spline will fit to said jumps. A minor example of this can be seen in Figure 3.3 for the month of December.

Remark 3.4.3. Since the at-the-money implied volatility is only observable for a finite number of maturities, a cubic Hermite spline is used to interpolate/extrapolate the other maturities.

Remark 3.4.4. Despite the omission of VIX Futures calibration, the initial forward variance curve ξ_0 will still be needed in Chapter 4 for SPX Options calibration, thus, the time will be taken to compute ξ_0 as detailed in Algorithm 3.4.5.

Calibration algorithm

Algorithm 3.4.5 (VIX Futures calibration algorithm in the ggBergomi model)**.**

1. Fit the cubic Hermite spline to SPX Option data;
2. compute the variance swap term structure $(\sigma_0(t)^2)_{t\geq 0}$;
3. compute the initial forward variance curve $\xi_0(t)$ using

$$\xi_0(t) \approx \sigma_0^2(t) + t\frac{\sigma_0^2(t+\epsilon) - \sigma_0^2(t-\epsilon)}{2\epsilon},$$

   with $\epsilon = 1E-8$;
4. minimise the objective function in Equation 3.4.

[1] CBOE VIX futures term structure: `https://www.cboe.com/tradable_products/vix/term_structure/`.

[2] CBOE SPX delayed option quotes: `https://www.cboe.com/delayed_quotes/spx/quote_table`.

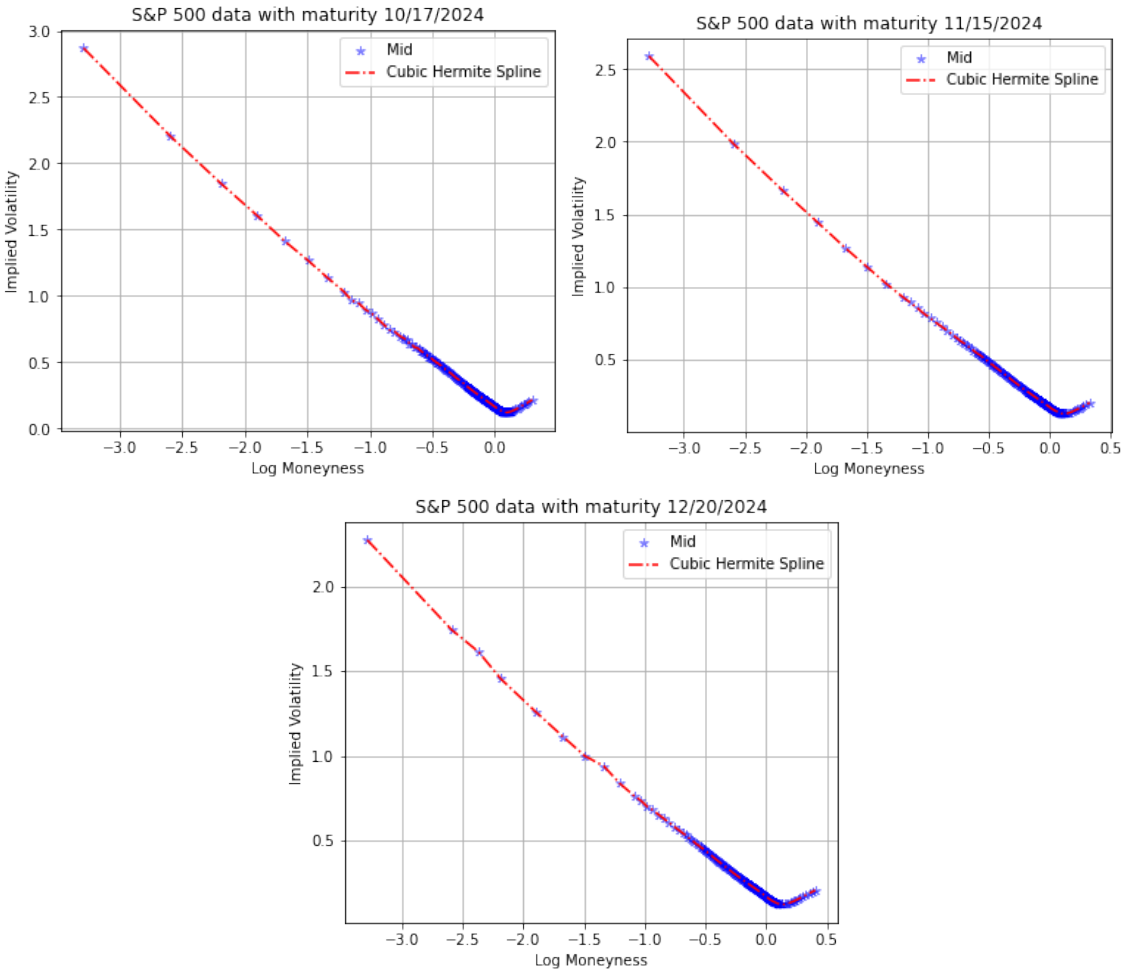

Figure 3.3: Cubic Hermite spline fit on 08/11/2024 using traded SPX Options.

Chapter 4

Pricing Methods in the Generalised Grey Bergomi Model

For the pricing scheme, a Cholesky decomposition is used. By definition, $\mathcal{V}_t$ has variance $\mathbb{V}[\mathcal{V}_t] = t^\alpha/\alpha$ and covariance

$$\mathbb{E}[\mathcal{V}_t\mathcal{V}_s] = \frac{t^{\frac{1}{2}(\alpha+1)}s^{\frac{1}{2}(\alpha-1)}}{\frac{1}{2}(\alpha+1)}{}_2F_1\left(-\frac{1}{2}(\alpha-1), 1, \frac{1}{2}(\alpha+3), \frac{t}{s}\right), \quad t < s, \tag{4.0.1}$$

with ${}_2F_1$ denoting the hypergeometric function. This can be verified via the following calculation:

$$\begin{aligned}
\mathbb{E}[\mathcal{V}_t\mathcal{V}_s] &= \int_0^t (t-u)^{\frac{1}{2}(\alpha-1)}(s-u)^{\frac{1}{2}(\alpha-1)}du \\
&= t^{\alpha-1}\int_0^t \left(1-\frac{u}{t}\right)^{\frac{1}{2}(\alpha-1)}\left(\frac{s}{t}-\frac{u}{t}\right)^{\frac{1}{2}(\alpha-1)}du \\
&= t^{\alpha}\int_0^1 (1-z)^{\frac{1}{2}(\alpha-1)}\left(\frac{s}{t}-z\right)^{\frac{1}{2}(\alpha-1)}dz \\
&= t^{\alpha}\left(\frac{s}{t}\right)^{\frac{1}{2}(\alpha-1)}\int_0^1 (1-z)^{\frac{1}{2}(\alpha-1)}\left(1-\frac{t}{s}z\right)^{\frac{1}{2}(\alpha-1)}dz \\
&= \frac{t^{\frac{1}{2}(\alpha+1)}s^{\frac{1}{2}(\alpha-1)}}{\frac{1}{2}(\alpha+1)}{}_2F_1\left(-\frac{1}{2}(\alpha-1), 1, \frac{1}{2}(\alpha+3), \frac{t}{s}\right).
\end{aligned}$$

Algorithm 4.0.1 (Simulation of the ggBergomi model)**.** Consider the grid $\mathcal{T} := \{t_i\}_{i=0,\dots,n_T}$, where $n_T := \lfloor nT \rfloor$, with n being the number of grid points per year and T denoting maturity.

1. Simulate the Volterra process $\mathcal{V}_t$ on the grid $\mathcal{T}$ using Equation (4.0.1);
2. compute the variance process $V_t = \xi_0(t)\mathcal{E}^{\blacklozenge}\left(\eta B_t^{\beta,\alpha}\right)$ for $t \in \mathcal{T}$;
3. back out the Brownian path from $\mathcal{V}_t$ to obtain $\{B_i\}_{i=0}^{n_T-1}$;
4. compute $\{B_i^\perp\}_{i=0}^{n_T-1}$, where $B^\perp \overset{(d)}{=} \mathcal{N}(0, 1/n_T)$ is an independent standard Gaussian sample, and correlate the two Brownian motions via $W_{t_i} - W_{t_{i-1}} = \rho B_{i-1} + \sqrt{1-\rho^2}B_{i-1}^\perp$;
5. simulate $S_{t_i} = \exp(X_{t_i})$ using a forward Euler scheme

$$X_{t_{i+1}} = X_{t_i} + \left(r - \frac{1}{2}V_{t_i}\right)(t_{i+1} - t_i) + \sqrt{V_{t_i}}(W_{t_{i+1}} - W_{t_i}), \text{ for } i = 0, \dots, n_T - 1;$$

6. compute the expectation by averaging the payoff of each path.

Remark 4.0.2. This is not the most computationally effective way to price under the gg-Bergomi model since the Cholesky scheme is slow and computationally expensive. Further discussion on this is provided in Chapter 5.

To gain some intuition as to how the parameter β impacts the implied volatilities generated in the ggBergomi, let

$$S_0 = 1, \quad \xi_0(t) = 0.235^2, \quad r = 0, \quad \alpha = 0.14, \quad \rho = 0, \quad \eta = 1.2287,$$

and consider the scenarios where 10^4 Monte Carlo simulations of the ggBergomi model are conducted on $t \in [0, 1]$ with $\beta \in \{0.25, 0.5, 0.75, 0.95, 0.99\}$. The implied volatilities of call options with maturity $T = 1$ can be observed in Figure 4.1. For curve-by-curve plots, the reader is referred to Appendix D.

Remark 4.0.3. From Figure 4.1, one can observe that as β decreases, the skew and curvature around the at-the-money point increases. Moreover, as β decreases, so does the level of the implied volatility smile. This allows the ggBergomi model to capture more general smiles in comparison to the rough Bergomi model. As a reminder, the skew and curvature at time zero are defined as

$$\mathcal{S}_T(k) \coloneqq |\partial_k \mathcal{I}_T(k)| \quad \text{and} \quad \mathcal{C}_T(k) \coloneqq \left|\partial_k^2 \mathcal{I}_T(k)\right|.$$

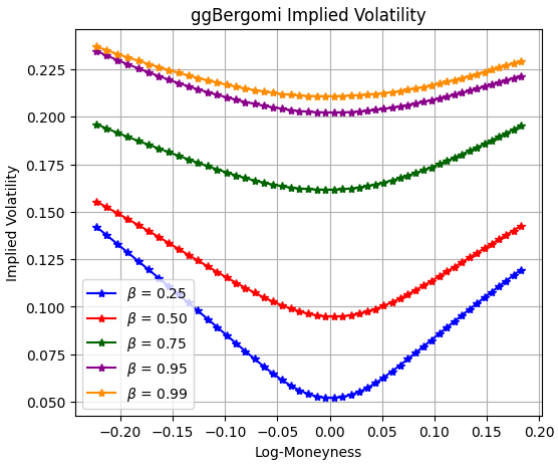

Figure 4.1: Implied Volatility Curves for $\beta \in \{0.25, 0.5, 0.75, 0.95, 0.99\}$.

4.1 Calibration of SPX Options via VIX Futures

Following Algorithm 3.4.5, calibrated values for α, β, η, and ξ_0 are obtained. The aim is to minimise the objective function

$$\mathcal{L}^{\mathrm{C}}(\beta, \eta, \rho) \coloneqq \sum_{j=1}^{L} \sum_{i=1}^{N} (\mathrm{C}_{T_{i,j}} - \mathrm{C}_{i,j}^{\mathrm{obs}})^2 \tag{4.1.1}$$

over (β, η, ρ), where $\mathrm{C}_{T_{i,j}}$ is the Call price given by the ggBergomi model computed using Algorithm 4.0.1 with maturity T_i and strike $K^{(j)}$. Meanwhile, $\mathrm{C}_{i,j}^{\mathrm{obs}}$ is the observed Call price at time T_i and strike $K^{(j)}$. The calibration algorithm is as follows:

Algorithm 4.1.1 (Calibration algorithm for SPX options via VIX Futures)**.**

1. Calibrate α, β, η, and ξ_0 via Algorithm 3.4.5;
2. compute M paths of the Volterra process $\{\mathcal{V}^{(u)}\}_{u=1}^{M}$, extract the Brownian motions $\{B^{(u)}\}_{u=1}^{M}$, and also compute the independent Brownian motions $\{B^{\perp(u)}\}_{u=1}^{M}$;
3. evaluate the Call prices in each calibration step:

$$\begin{aligned} V_t^{(u)} &= \xi_0(t)\mathcal{E}^{\blacklozenge}\left(\eta B_t^{\beta,\alpha}\right), \quad u = 1, \dots, M, \\ W^{(u)} &= \rho B^{(u)} + \sqrt{1-\rho^2}B^{\perp(u)}, \quad u = 1, \dots, M, \\ S_{t+\Delta}^{(u)} &= S_t^{(u)} + S_t^{(u)}\sqrt{V_t^{(u)}}\left(W_{t+\Delta}^{(u)} - W_t^{(u)}\right), \quad u = 1, \dots, M; \end{aligned}$$

4. compute the Call price for each maturity and each strike

$$C_{T_i,j} = \frac{1}{M}\sum_{u=1}^{M}\left(S_{T_i}^{(u)} - K^{(j)}\right)^{+} \quad \text{for } i = 1, \dots, N \text{ and } i = 1, \dots, L;$$

5. minimise the objective function in Equation (4.1.1).

Remark 4.1.2. As in the rough Bergomi model, the initial forward variance curve ξ_0 plays a very important part in the implied volatilities generated by the ggBergomi model [27]. For an accurate fit to market-observed implied volatilities, the forward variance must be estimated precisely. A relatively simple way of doing so is provided in Algorithm 3.4.5, however, there are most certainly better ways of estimating this quantity.

Remark 4.1.3. From a less rigorous standpoint and from more of a philosophical one, given the role that β plays in determining the shape of the implied volatility curve (for example, see Figure 4.1), the following questions naturally arise when calibrating β:

1. how greatly does the calibrated parameter β differ between VIX and SPX calibration?
2. if there is a difference between the two, then what does that mean in a practical sense? Is there a possible arbitrage opportunity as speculated in [27] when there is a difference in η?

Remark 4.1.4. Due to VIX Futures calibration being computationally infeasible without a closed-form formula for Futures prices, no comments can be made on the difference in η and β between VIX and SPX calibration.

Numerical results

For numerical experiments, the ggBergomi model is calibrated on 08/11/2024 with the assumption that $\alpha = 0.14$ since VIX Futures calibration was omitted. Figure 4.2 and Figure 4.3 show calibrated and non-calibrated results, respectively, where the parameter values are as in Table 4.1.

	β	η	ρ
Calibrated	0.5	1	0.0412
Non-Calibrated	0.8	2	-0.001

Table 4.1: Calibrated vs Non-Calibrated Parameters.

Remark 4.1.5. It is worth noting that due to the misspecified parameter α (and potentially ξ_0), the ggBergomi model cannot correctly match the SPX Option market prices, giving rise to the absolute errors observed in Figure 4.2 and Figure 4.3. The magnitude of these errors eliminates the possibility of comparing the implied volatility curves generated.

Remark 4.1.6. Since there are considerably more quoted options around the at-the-money mark, solving Equation (4.1.1) without having calibrated first to VIX Futures will naturally lead to a model which only fits well around the at-the-money point. In the case of Figure 4.2, one can see that the neighborhood around the at-the-money point where the error is reasonable is far too small, thus, emphasising the fact that the parameters calibrated through VIX Futures are crucial to obtain a reasonable fit.

Remark 4.1.7. With an initial guess of $(\beta, \eta, \rho) = (0.5, 1, 0)$ the optimisers available in Python all converge to near the initial guess, thus, suggesting that the loss surface isn't steep enough for the optimiser to make any progress. A potential work-around is to consider a weighted optimisation problem such that Remark 4.1.6 is also addressed. Furthermore, Figure 4.3 suggests that this optimisation problem is solvable and will lead to promising implied volatility fits.

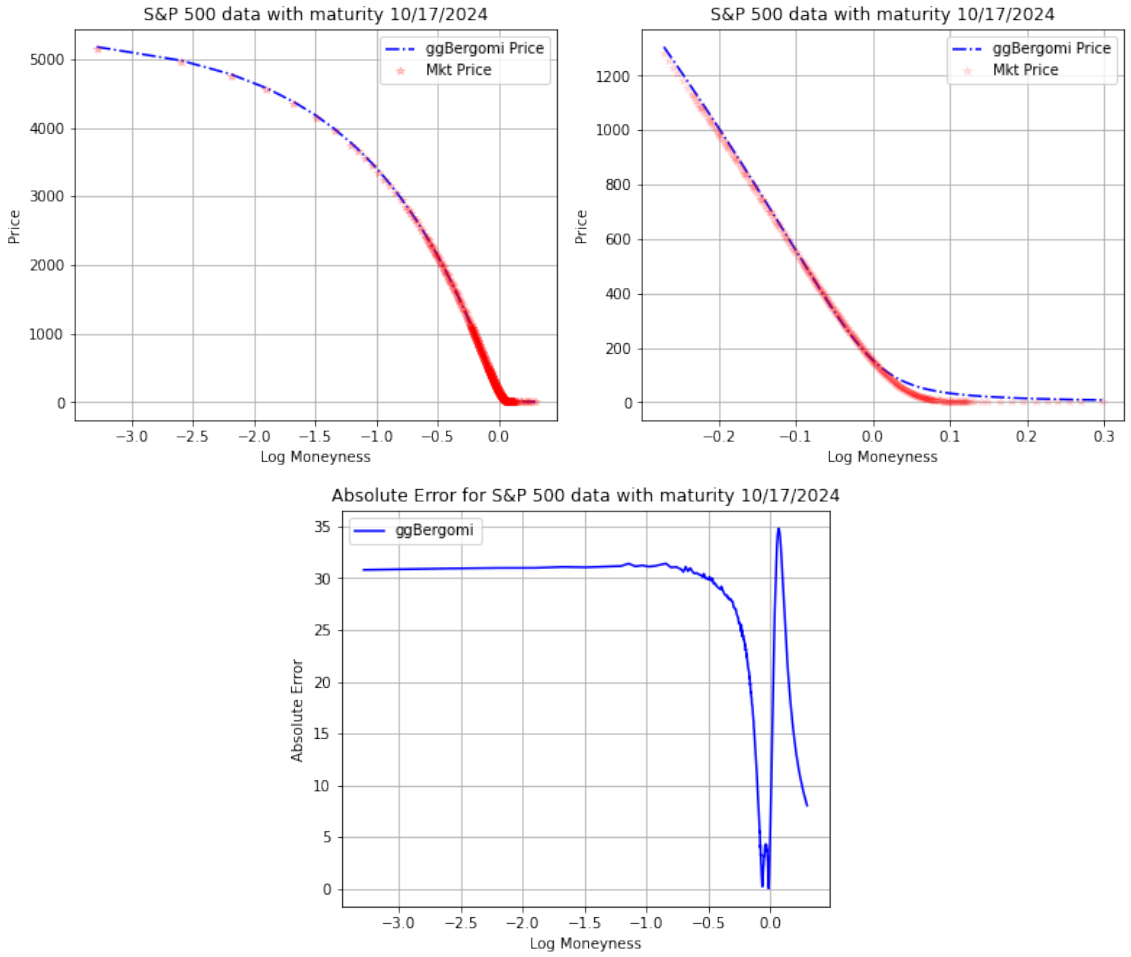

Figure 4.2: Calibrated SPX Option prices under the ggBergomi model in comparison to market data with $(\beta, \eta, \rho) = (0.5, 1, 0.0412)$ on 08/11/2024.

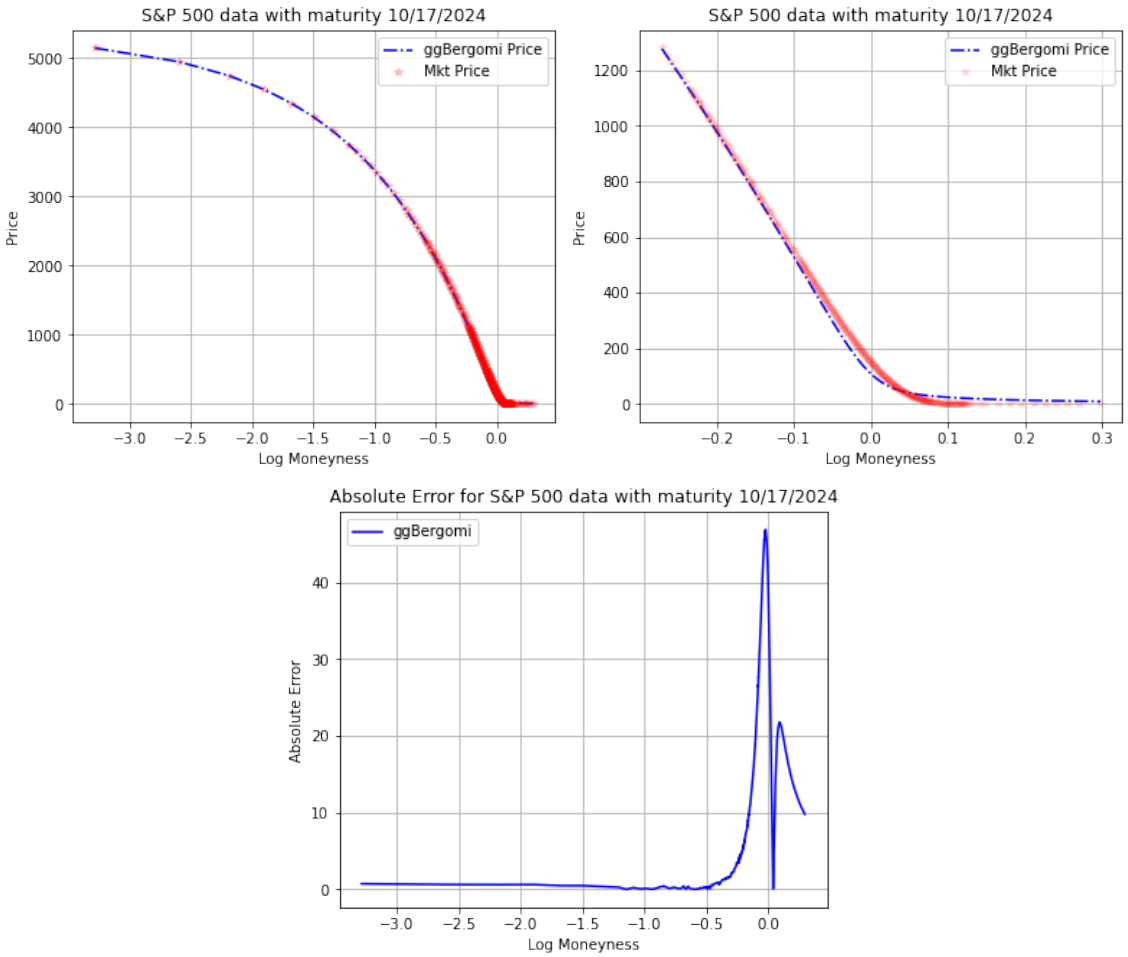

Figure 4.3: Non-calibrated SPX Option prices under the ggBergomi model in comparison to market data with $(\beta, \eta, \rho) = (0.8, 2, -0.001)$ on 08/11/2024.

Chapter 5

Conclusion and Future Work

After much groundwork such as M-Wright variate generation through fractional Poisson processes and understanding precisely the concept of "generalised" grey noise, the ggBergomi model was introduced as a natural generalisation of the rough Bergomi model. Under the ggBergomi model, the discounted stock price process was shown to be a martingale in Chapter 3, thus, importantly eliminating arbitrage in derivative prices generated. Chapter 3 also characterised the forward variance under the ggBergomi model whilst providing upper and lower bounds for VIX Futures prices. Additionally, using a truncated Cholesky scheme, numerical experiments were conducted to test the upper and lower bounds and also to compare VIX Futures prices under the ggBergomi model and rough Bergomi model.

Despite the ggBergomi model being far from the finished product in terms of joint calibration (due to the lack of VIX Future and Option pricing formulae), the superiority of the ggBergomi model over the rough Bergomi model in terms of flexibility was showcased in Chapter 3 and Chapter 4 through pricing VIX Futures and Vanilla Options. In particular, for Vanilla Options, the added degree of freedom with the parameter β allows for direct control over the level, skew, and curvature of the implied volatility curve (as showcased in Figure 4.1).

5.1 Future Work

Due to time constraints, all avenues of possible research were not explored, leaving much for future research. The following subsections outline these problems and potential ways to solve them.

5.1.1 VIX Futures and Options

In the case of VIX Futures/Options pricing, a significant speed-up can be achieved by developing closed formulae. This allows for calibration times orders of magnitude smaller than brute force Monte Carlo simulations, thus, making VIX calibration feasible. The problem in both cases boils down to determining the distribution of

$$\Delta \operatorname{VIX}_T^2 = \int_T^{T+\Delta} \xi_T(s) ds,$$

which is effectively finding the distribution of the sum of forward variances. When $\beta = 1$ in the ggBergomi model, one can make use of the fact that asymptotically the sum of log-normal random variables is also log-normal [17]. The problem isn't trivial for $\beta \in (0, 1)$. Approximations inspired by the one in [5] might be fruitful. In light of this, a direct way of tackling the problem is by using an exact/approximated conditioned density (for reference see [5, 27]) and integrating against the one-sided M-Wright density. Of

course, the feasibility of evaluating this integral is yet to be determined, but this yields the approximated joint density for ΔVIX^2 from which VIX Futures can be calculated since VIX is non-negative.

Remark 5.1.1. If an approximation similar in flavour to [5] is obtained then an immediate approximation to the VVIX process is obtained. One reason this is of benefit is so that one can test if the empirical relationship between VIX and VVIX (for reference see [8]) is replicated under the ggBergomi model. Moreover, it would lead to a better insight in relation to Remark 2.0.1.

5.1.2 Pricing under ggBergomi

Hybrid Scheme

Using a Cholesky scheme to simulate the Volterra process is slow and expensive. For an $n \times n$ matrix, the Cholesky decomposition has complexity $\mathcal{O}(n^3)$. This can be improved by following [27]. The hybrid scheme from [6] can be used instead, making the pricing scheme more efficient as the complexity to simulate the Volterra process is reduced to complexity $\mathcal{O}(n \log n)$. For reference, the hybrid scheme is provided in Appendix E.

Markovian Approximation

Due to the non-Markovian nature of the variance process in the ggBergomi model, simulation schemes are computationally expensive and slow. A workaround is to consider a Markovian approximation to the Volterra process [4, 13].

In the case of the power law kernel $K(t) := \frac{t^{\frac{1}{2}(\alpha-1)}}{\Gamma(\frac{1}{2}(\alpha+1))}$

$$K(t) = \int_0^\infty e^{-tx}\mu(dx), \quad \mu(x) := \frac{L_\alpha dx}{x^{\frac{1}{2}(\alpha+1)}}, \quad L_\alpha := \frac{1}{\Gamma(\frac{1}{2}(\alpha+1))\Gamma(\frac{1}{2}(1-\alpha))}.$$

Hence, from the stochastic Fubini theorem, one obtains

$$\int_0^t K(t-s)dB_s = \int_0^\infty \int_0^t e^{-(t-s)x} dB_s \mu(dx) = \int_0^\infty Y_t^x \mu(dx),$$

where $Y_t^x := \int_0^t e^{-(t-s)x} dB_s$. Note that Y_t^x is an Ornstein-Uhlenbeck process which is indeed a Markov process. Approximating the kernel $K(t)$ by finite sums yields

$$K(t) = \int_0^\infty e^{-tx}\mu(dx) \approx \sum_{i=0}^N w_i^N e^{-x_i^N t},$$

where $(w_i^N)_{i=1}^N$ are positive weights and $(x_i^N)_{i=1}^N$ are mean-reverting speeds. Applying this to the ggBergomi model results in the Markovian approximations S^N and V^N,

$$S_t^N = S_0^N \exp\left\{-\frac{1}{2}\int_0^t V_s^N ds + \int_0^t \sqrt{V_s^N}(\rho dB_s + \sqrt{1-\rho^2} dB_s^\perp)\right\},$$
$$V_t^N = \xi_0(t)\mathcal{E}_\beta\left(\frac{\eta^2 C_{\frac{\alpha}{2}}^2 t^\alpha}{2\alpha}\right)^{-1} \exp\left\{\eta\sqrt{Y_\beta}\int_0^t \sum_{i=0}^N w_i^N e^{-x_i^N(t-s)} dB_s\right\},$$

where $S_0^N = S_0 = 1$ and $V_0^N = V_0 = 0$. Given the positive weights $(w_i^N)_{i=1}^N$ and the mean-reverting speeds $(x_i^N)_{i=1}^N$, one can simulate the Markovian approximation of the ggBergomi model.

Carefully choosing weights and mean-reverting speeds can drastically improve the value of N one needs in order to obtain a given accuracy. An example of this can be seen in comparing the methodology in [4] and [40], where in [4] one can afford to use a considerably smaller N, thus, decreasing simulation times.

Remark 5.1.2. The Markovian approximation scheme can potentially be improved by using the Clenshaw–Curtis quadrature scheme. The Clenshaw–Curtis quadrature scheme is similar to the Gaussian quadrature scheme where in some cases the spectral accuracy is the same, however, the grid points and weights take $\mathcal{O}(N \log N)$ time to evaluate instead of $\mathcal{O}(N^2)$ time. Conditions as to when the Clenshaw–Curtis quadrature scheme has the same spectral accuracy as the Gaussian quadrature scheme are formalised in [39, Theorem 4.5, Theorem 5.1].

It suffices to check that the integrand of interest satisfies the following conditions:

1. $f \in \mathcal{C}([-1,1])$;
2. $f, f^{(1)}, \ldots, f^{(k-1)}$ are absolutely continuous on $[-1,1]$;
3. $||f^{(k)}||_T = \left|\left|f^{(k+1)}(x)/\sqrt{1-x^2}\right|\right|_1 = K < \infty$ for $k \geq 1$ where the norm used is the Chebyshev-weighted 1-norm and is defined via a Stieltjes integral for any function of bounded variation.

If the three conditions hold, then for all sufficiently large N, the error of the Clenshaw–Curtis quadrature scheme is of order $\mathcal{O}(K/[k(2N-1+k)^k])$.

The scheme will be applied to the compact intervals $[\upsilon_i, \upsilon_{i+1}]$ for $i = 0, \ldots, n$ found in [4] and subsequently the integrals of interest (ignoring scaling factors) are

$$\begin{aligned}\int_{[\upsilon_i,\upsilon_{i+1}]} e^{-xt} x^{-\frac{1}{2}(\alpha+1)} dx &= \frac{\upsilon_{i+1}-\upsilon_i}{2} \exp\left(-\frac{\upsilon_{i+1}+\upsilon_i}{2}t\right) \int_{-1}^{1} \exp\left(-\frac{\upsilon_{i+1}-\upsilon_i}{2}ut\right) \\ &\quad \left(\frac{\upsilon_{i+1}-\upsilon_i}{2}u + \frac{\upsilon_{i+1}+\upsilon_i}{2}\right)^{-\frac{1}{2}(\alpha+1)} du \\ &= \frac{\upsilon_{i+1}-\upsilon_i}{2} \exp\left(-\frac{\upsilon_{i+1}+\upsilon_i}{2}t\right) \int_{-1}^{1} f(u) du,\end{aligned}$$

where $f(u) := \exp\left(-\frac{\upsilon_{i+1}-\upsilon_i}{2}ut\right)\left(\frac{\upsilon_{i+1}-\upsilon_i}{2}u + \frac{\upsilon_{i+1}+\upsilon_i}{2}\right)^{-\frac{1}{2}(\alpha+1)}$ with $g(u) := \exp\left(-\frac{\upsilon_{i+1}-\upsilon_i}{2}ut\right)$ and $h(u) := \left(\frac{\upsilon_{i+1}-\upsilon_i}{2}u + \frac{\upsilon_{i+1}+\upsilon_i}{2}\right)^{-\frac{1}{2}(\alpha+1)}$. Since $\upsilon_0 > 0$, f satisfies the first and second conditions. Moreover, $f \in \mathcal{C}^\infty([-1,1])$. For the third condition, using the general Leibniz product rule

$$f^{(k)}(u) = \sum_{j=0}^{k} \binom{k}{j} g^{(k-j)}(u) h^{(j)}(u),$$

where for $k \geq 1$

$$g^{(k)}(u) := \left(-\frac{\upsilon_{i+1}-\upsilon_i}{2}t\right)^k \exp\left(-\frac{\upsilon_{i+1}-\upsilon_i}{2}ut\right),$$

and

$$h^{(k)}(u) := \left[\prod_{j=1}^{k}\left(-\frac{1}{2}(\alpha+1)-j+1\right)\right]\left(\frac{\upsilon_{i+1}-\upsilon_i}{2}\right)^k \left(\frac{\upsilon_{i+1}-\upsilon_i}{2}u + \frac{\upsilon_{i+1}+\upsilon_i}{2}\right)^{-\frac{1}{2}(\alpha+1)-k}.$$

Therefore,

$$||f^{(k)}||_T = \int_{-1}^{1} \frac{\left|f^{(k+1)}(x)\right|}{\sqrt{1-x^2}} dx \leq \int_{-1}^{1} \frac{\sum_{j=0}^{k+1} \binom{k}{j} \left|g^{(k-j)}(x)\right| \left|h^{(j)}(x)\right|}{\sqrt{1-x^2}} dx.$$

Splitting the integral on the positive and negative part of the interval yields two cases. For the case where $u \in [0,1]$, one can make use of the fact that

$$\left(\frac{\upsilon_{i+1}-\upsilon_i}{2}u + \frac{\upsilon_{i+1}+\upsilon_i}{2}\right)^{-x} \leq \left(\frac{\upsilon_{i+1}+\upsilon_i}{2}\right)^{-x}, \quad x \in \mathbb{R}_{\geq 0},$$

and thus, $\left|h^{(k)}\right|$ is always bounded. For the negative part of the integral one can make use of the fact that for $u \in [-1,0]$

$$\left(\frac{\upsilon_{i+1}-\upsilon_i}{2}u + \frac{\upsilon_{i+1}+\upsilon_i}{2}\right)^{-x} \leq \upsilon_i^{-x}, \quad x \in \mathbb{R}_{\geq 0}.$$

Again, $\left|h^{(k)}\right|$ is always bounded. Note that for both cases $\left|g^{(k)}\right|$ is trivially bounded as its maximum is achieved on the left of each interval. Therefore, for all $k \geq 1$ the third condition holds, thus, by [39, Theorem 4.5, Theorem 5.1] the Clenshaw–Curtis quadrature scheme has the same spectral accuracy as the Gaussian quadrature scheme.

Thus, if a result in the same spirit as [4, Lemma A.1] can be proven for the Clenshaw–Curtis grid points, then a slightly more efficient scheme is obtained. By [39, Theorem 4.5, Theorem 5.1] it seems natural that [4, Lemma A.1] holds for the Clenshaw-Curtis grid points, however, this needs to be proved rigorously.

5.1.3 Calibrating with Deep Learning

Inspired by [26, 38], a Deep Learning approach can be taken to drastically improve the calibration time of the ggBergomi model. Note that this approach is not feasible unless closed form formulae for VIX Futures and Options are derived, otherwise, a synthetic dataset cannot be constructed for VIX Futures or Options calibration.

5.1.4 Skew-Stickiness-Ratio (SRR)

Joint calibration is not the only thing a model should be concerned with, other metrics such as SRR must also be considered. Let $[X,Y]_{[t,s]}$ denote the quadratic covariation between two Itô processes X and Y on the interval $[t,s]$. Recall that SRR with time to maturity τ is defined as [9]

$$\mathcal{R}_t(\tau) := \frac{1}{\mathcal{S}_t(\tau)} \frac{\frac{\mathrm{d}}{\mathrm{d}s}[\log S_\cdot, \sigma_\cdot(\tau)]_{[t,s]}|_{s=t}}{\frac{\mathrm{d}}{\mathrm{d}s}[\log S_\cdot]_{[t,s]}|_{s=t}},$$

where $\sigma_\cdot$ and $\mathcal{S}_\cdot$ denote the at-the-money-forward implied volatility and skew, respectively. An analysis comparing the market SRR and SRR under the ggBergomi must also be conducted. This should be relatively straightforward given the two recent publications [9, 21].

Appendix A

M-Wright Variate Generation

A.1 Renewal Theory

Summarising [30], let $N(t)$ be a counting process for the number of events up to time $t > 0$. Renewal processes are a class of counting processes where the time between successive events, $T_1, T_2, \ldots$ are i.i.d. random variables. The time between successive events is referred to as waiting times and renewal times are defined as

$$t_0 = 0, \quad t_k = \sum_{j=1}^{k} T_j, \quad k \geq 1.$$

Suppose that the waiting times are distributed like T, define the cumulative distribution function (cdf)

$$\Phi(t) := \mathbb{P}(T \leq t),$$

where Φ is assumed to be absolutely continuous in order to define its probability density function (pdf)

$$\phi(t) := \Phi'(t).$$

For convenience define $\Psi(t) := 1 - \Phi(t)$. Now suppose that one is interested in making conclusions about the renewal times. Let

$$F_k(t) := \mathbb{P}(t_k \leq t), \quad f_k(t) := F_k'(t), \quad k \geq 1.$$

In the case of a sum of i.i.d. exponential random variables, the function F_k is the Erlang cdf and f_k is referred to as the Erlang pdf. With this and the assumption that the waiting times are i.i.d. random variables, one has that the pdf of $N(t)$ is

$$v_k(t) := \mathbb{P}(N(t) = k) = \mathbb{P}(t_k \leq t, t_{k+1} > t) = \int_0^t f_k(s)\Psi(t-s)ds.$$

Remark A.1.1. A Poisson process (with $\lambda > 0$) is the most renowned renewal process where in the notation given

$$\Phi(t) = e^{-\lambda t}, \quad \phi(t) = \lambda e^{-\lambda t}, \quad t \geq 0,$$

and

$$v_k(t) = \frac{(\lambda t)^k}{k!} e^{-\lambda t}, \quad t \geq 0, \quad k \in \mathbb{Z}_{\geq 0}.$$

The Erlang pdf and cdf are

$$f_k(t) = \lambda \frac{(\lambda t)^{k-1}}{(k-1)!} e^{-\lambda t}, \quad F_k(t) = \sum_{n=k}^{\infty} \frac{(\lambda t)^n}{n!} e^{-\lambda t}, \quad t \geq 0, \quad k \in \mathbb{Z}_{\geq 0}.$$

As in [30] a fractional generalisation of the Poisson process can be constructed. For a Poisson process, it is known that Ψ satisfies the following ODE:

$$\Psi'(t) = -\lambda\Psi(t), \quad t \geq 0, \quad \Psi(0^+) = 1.$$

One can generalise the ODE by replacing the derivative by a Caputo fractional derivative of order $\beta \in (0, 1]$, where a Caputo derivative of order $\beta \in (0, 1]$ of a "well-behaved" function f is defined as [12]

$${}_tD_*^\beta := \begin{cases} \dfrac{1}{\Gamma(1-\beta)} \displaystyle\int_0^t \frac{f^{(1)}(\tau)}{(t-\tau)^\beta} d\tau, & 0 < \beta < 1, \\ f'(t), & \beta = 1. \end{cases}$$

Remark A.1.2. The Laplace transform of the Caputo derivative of a function f is

$$\mathcal{L}\{{}_tD_*^\beta f(t); s\} = s^\beta \widetilde{f}(s) - s^{\beta-1} f(0^+),$$

where $\widetilde{f}$ is the Laplace transform of f.

Assuming $\lambda = 1$, this results in

$${}_tD_*^\beta \Psi(t) = -\Psi(t), \quad t \geq 0, \quad 0 < \beta \leq 1, \quad \Psi(0^+) = 1.$$

By Laplace transforms, the solution to the generalised ODE is

$$\Psi(t) = \mathcal{E}_\beta(-t^\beta).$$

For a generalisation of the quantities in Remark A.1.2, the Laplace transform is given [35, Equation (1.80)]

$$\mathcal{L}\{t^{\beta k}\mathcal{E}_\beta^{(k)}(-t^\beta); s\} = \frac{k! s^{\beta-1}}{(1+s^\beta)^{k+1}}, \quad \beta > 0, \quad k = 0, 1, \ldots,$$

with $\mathcal{E}_\beta^{(k)}(z) := \frac{d^k}{dz^k}\mathcal{E}_\beta(z)$. Thus, after some computations (see [30] for further details), the Erlang pdf and cdf are

$$f_k(t) = \beta \frac{(t)^{\beta k-1}}{(k-1)!}\mathcal{E}_\beta^{(k)}(-t^\beta), \quad F_k(t) = \sum_{n=k}^{\infty} \frac{t^{\beta n}}{(n)!}\mathcal{E}_\beta^{(k)}(-t^\beta), \quad t \geq 0, \quad 0 < \beta < 1, \quad k \in \mathbb{Z}_{\geq 0}.$$

This results in the pdf of $N(t)$,

$$v_k(t) = \frac{t^{k\beta}}{k!}\mathcal{E}_\beta^{(k)}(-t^\beta), \quad t \geq 0, \quad 0 < \beta < 1, \quad k \in \mathbb{Z}_{\geq 0},$$

which is a generalisation of the Poisson distribution (with parameter t), referred to as a β-fractional Possion (β-fP) distribution.

A.2 Stable Distributions

Definition A.2.1 (Stable Distribution [29])**.** A random variable X is said to have a stable distribution if, for any $n \geq 2$, there is a positive number c_n and a real number d_n such that

$$\sum_{i=1}^{n} X_i \overset{(d)}{=} c_n X + d_n,$$

where $X_1, \ldots, X_n$ are i.i.d random variables.

Remark A.2.2. From [19, Theorem 1, Chapter 6], the constants from Definition A.2.1 are of the form

$$c_n = n^{1/\beta}, \quad \beta \in (0, 2].$$

The parameter β is called the characteristic exponent or the index of stability of the distribution. Note that in the case of this thesis, the range of β will be limited to $(0, 1]$ due to the Caputo derivative used to construct the β-fP distribution.

Definition A.2.3 (β-Stable Distribution [29])**.** A random variable X has a β-stable distribution if X has a stable probability distribution with characteristic exponent β.

A.3 One-Sided M-Wright Variate Generation

From Chapter 1, the Laplace transform of the M-Wright density is

$$\phi_Z(\lambda) = \int_0^\infty e^{-\lambda z} \mathcal{M}_\beta(-z) dz = \mathcal{E}_\beta(-\lambda).$$

Following the analysis of [11], let $N_\beta(t)$ be the number of events that have occurred up until time $t > 0$ in the β-fP process with intensity $\eta > 0$. Now consider the scaled β-fP random variable

$$Z_\beta = \frac{N_\beta(t)}{\eta t^\beta}.$$

It can be shown that $\phi_{Z_\beta}(\lambda) \to \phi_Z(\lambda)$ as $t \to \infty$, where ϕ_{Z_β} is the Laplace transform of the density of Z_β. Since the Laplace transform of a function is unique, then the limiting distribution of the scaled β-fP random variable Z_β converges to the M-Wright function as $t \to \infty$. Furthermore, one can write the limiting distribution of Z_β and $\mathcal{M}_\beta$ as a one-sided β-stable density $s^{(\beta)}(\xi)$ with Laplace transform $\exp\left(-\lambda^\beta\right)$ as

$$\mathcal{M}_\beta(-z) = f_\beta(z) = \frac{z^{-1-1/\beta}}{\beta} s^{(\beta)}(z^{-1/\beta}).$$

By a change of variables $r = z^{-1/\beta}$, one obtains

$$\frac{\beta}{r^{\beta+1}} \mathcal{M}_\beta(-r^{-\beta}) = \frac{\beta}{r^{\beta+1}} f_\beta(r^{-\beta}) = s^{(\beta)}(r).$$

This results in

$$Z \overset{(d)}{=} R^{-\beta},$$

where Z is a one-side M-wright random variable and R is a random variable from the one-sided β-stable distribution $s^{(\alpha)}(r)$. Converting the implementation of this in R [10] to Python allows for the following variate generation in Figure A.1.

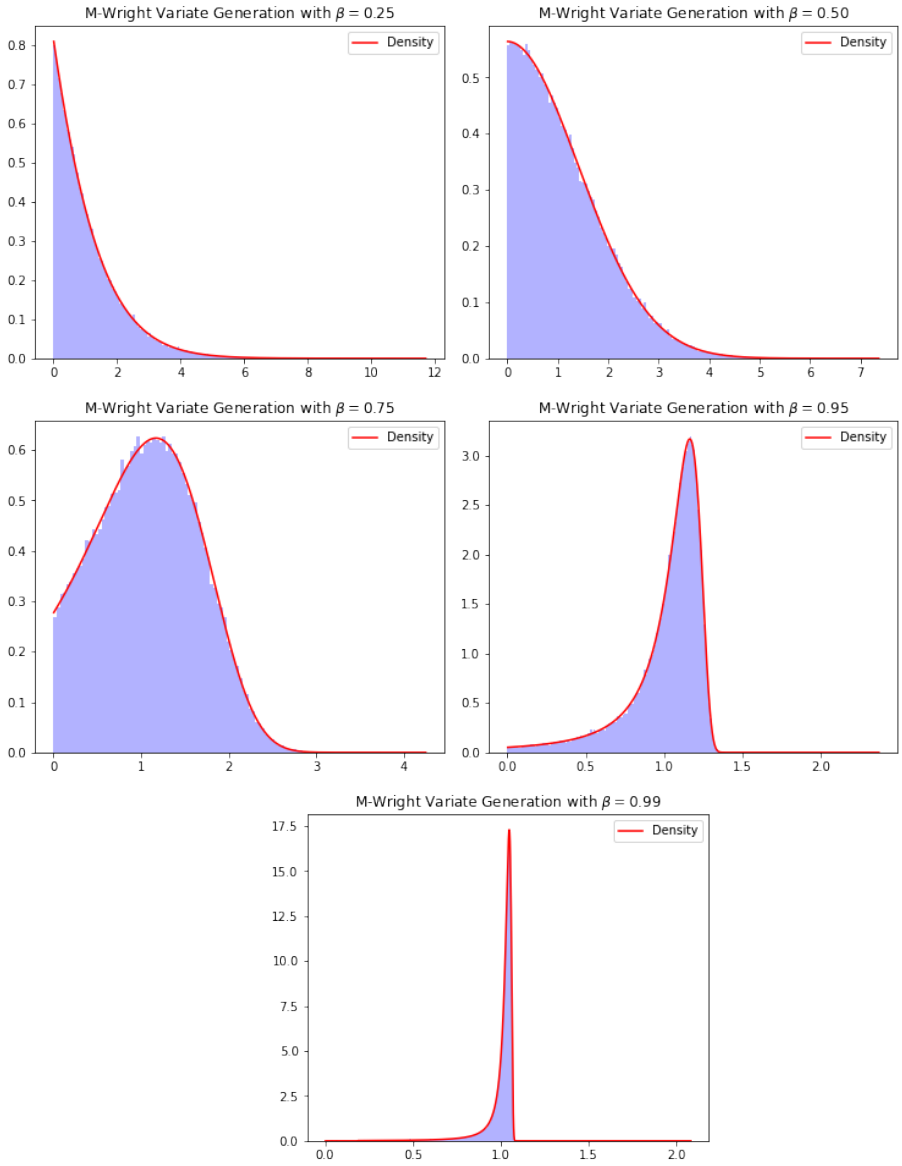

Figure A.1: M-Wright density and 10^5 M-Wright variates for $\beta = 0.25, 0.5, 0.75, 0.95, 0.99$.

Appendix B

Technical Proofs

Lemma B.0.1. *Let X, Y be two random variables on $(\Omega, \mathcal{F})$ such that $X, Y \neq 0$ a.s.. Then, it holds for the generated sigma-algebra of the product that*

$$\sigma(X \cdot Y) \subseteq \sigma(X) \vee \sigma(Y).$$

Proof. Let $f(x, y) = x \cdot y$ and $\mathcal{B} \subseteq \mathcal{F}$ any Borel-measurable set. Then, since any continuous function is Borel measurable, $f^{-1}(\mathcal{B})$ is a Borel set

$$\{\omega : (X \cdot Y)(\omega) \in \mathcal{B}\} = \{\omega : f(X(\omega), Y(\omega)) \in \mathcal{B}\} = \left\{\omega : (X(\omega), Y(\omega)) \in f^{-1}(\mathcal{B})\right\}.$$

Therefore, f is $\sigma(X) \vee \sigma(Y)$-measurable. □

B.1 Proof of Thoerem 3.1.6

Proof. Using ggRLBm, the discounted dynamics of $(S_t)_{t=0}^{\infty}$ are

$$\frac{dS_t}{S_t} = \sqrt{V_t}(\rho dB_t + \sqrt{1-\rho^2}dW_t) = \sigma(t, B_t^{\frac{\alpha}{2}})(\rho dB_t + \sqrt{1-\rho^2}dW_t),\ S_0 = 1,$$

$$V_t = \xi_0(t)\mathcal{E}(\eta B_{\mathrm{RL},t}^{\beta,\alpha}),\ V_0 > 0.$$

Furthermore, by Lemma 2, $B_{\mathrm{RL},t}^{\beta,\alpha} \overset{(d)}{=} \sqrt{Y_\beta} B_t^{\frac{\alpha}{2}}$, with

$$B_t^{\frac{\alpha}{2}} = C_{\frac{\alpha}{2}} \int_0^t (t-s)^{\frac{1}{2}(\alpha-1)} dB_s,$$

where $C_{\frac{\alpha}{2}} := \frac{1}{\Gamma(\frac{1}{2}(1+\alpha))}$. Clearly, $(S_t)_{t=0}^{\infty}$ is a non-negative local martingale (hence supermartingale), it will be a martingale on $[0, T]$ if and only if $\mathbb{E}[S_T] = \mathbb{E}[\mathbb{E}[S_T|Y_\beta]] = S_0$. Now define $\tau_n := \inf\{t > 0, B_t^{\frac{\alpha}{2}} = n\}$ and since σ is bounded on $[0, T] \times (-\infty, n]$, one has that

$$S_0 = \mathbb{E}[\mathbb{E}[S_{T\wedge\tau_n}|Y_\beta]] = \mathbb{E}[\mathbb{E}[S_T \mathbb{1}_{\{T\leq\tau_n\}}|Y_\beta]] + \mathbb{E}[\mathbb{E}[S_{\tau_n} \mathbb{1}_{\{\tau_n\leq T\}}|Y_\beta]].$$

Taking $n \to \infty$ yields

$$S_0 - \mathbb{E}[\mathbb{E}[S_T|Y_\beta]] = \lim_{n\to\infty} \mathbb{E}[\mathbb{E}[S_{\tau_n} \mathbb{1}_{\{\tau_n\leq T\}}|Y_\beta]].$$

Using Girsanov's theorem, one can write

$$\mathbb{E}[\mathbb{E}[S_{\tau_n} \mathbb{1}_{\{\tau_n\leq T\}}|Y_\beta]] = S_0 \mathbb{E}[\hat{\mathbb{P}}_n(\tau_n \leq T)],$$

where $\hat{\mathbb{P}}_n$ is a random measure (conditional on Y_β) chosen such that

$$\hat{W}_t^{(n)} = W_t - \int_0^{t\wedge\tau_n} \sigma(t, B_t^{\frac{\alpha}{2}})ds,$$

is a Brownian motion under $\hat{\mathbb{P}}_n$. Note that for $t \leq \tau_n$, one has

$$\begin{aligned} B_t^{\frac{\alpha}{2}} &= C_{\frac{\alpha}{2}} \int_0^t (t-s)^{\frac{1}{2}(\alpha-1)} \left(d\hat{B}_s^{(n)} + \rho\sigma(s, B_s^{\frac{\alpha}{2}})ds \right), \\ &= \hat{B}_t^{\frac{\alpha}{2}} + C_{\frac{\alpha}{2}} \int_0^t (t-s)^{\frac{1}{2}(\alpha-1)} \rho\sigma(s, B_s^{\frac{\alpha}{2}})ds, \end{aligned}$$

where $\hat{B}_t^{(n)}$ is a $\hat{\mathbb{P}}_n$-Brownian motion and

$$\hat{B}_t^{\frac{\alpha}{2}} := C_{\frac{\alpha}{2}} \int_0^t (t-s)^{\frac{1}{2}(\alpha-1)} d\hat{B}_s^{(n)}.$$

In the case that $\rho \leq 0$, $B_t^{\frac{\alpha}{2}} \leq \hat{B}_t^{\frac{\alpha}{2}}$ for $t \leq \tau_n$; moreover, one has $\tau_n \geq \tau_n^0 := \inf\{t > 0, \hat{B}_t^{\frac{\alpha}{2}} = n\}$. In addition, by Dominated Convergence and using the fact that $\hat{B}^{(n)}$ is a $\hat{\mathbb{P}}_n$-Brownian motion

$$\lim_{n\to\infty} \mathbb{E}\left[\hat{\mathbb{P}}_n\left(\tau_n^0 \leq T\right)\right] = \mathbb{E}\left[\lim_{n\to\infty} \hat{\mathbb{P}}_n\left(\tau_n^0 \leq T\right)\right] = \mathbb{E}\left[\lim_{n\to\infty} \mathbb{P}\left(\sup_{t\in[0,T]} B_t^{\frac{\alpha}{2}} \geq n\right)\right] = 0.$$

Thus, it follows that

$$S_0 - \mathbb{E}[\mathbb{E}[S_T|Y_\beta]] = 0,$$

in other words, S is a martingale if $\rho \leq 0$.

□

Appendix C

Preliminaries for Grey Noises

In this chapter, a summary of introductory concepts from [32] is provided. Let X be a topological vector space and denote X' as the dual space of X. Let $\langle \cdot, \cdot \rangle$ be the natural bilinear pairing between X and X', where X' is equipped with the weak topology.

Definition C.0.1. A Hilbert-Schmidt operator is a bounded operator A defined on a Hilbert space such that there exists an orthonormal basis $\{e_i\}_{i \in I}$ of H such that $\sum_{i \in I} ||Ae_i||^2 < \infty$.

With this, the notion of a nuclear space can be defined. Note that these kinds of spaces and the upcoming results are central to this thesis and the reason why is apparent in Chapter 3.

Definition C.0.2. A topological vector space X, with the topology defined by a family of Hilbert-norms is nuclear if, for any Hilbert norm $|| \cdot ||_p$, there exists a larger norm $|| \cdot ||_q$ such that the inclusion map $X_q \hookrightarrow X_p$ is a Hilbert-Schmidt operator.

Theorem C.0.3 (Minlos' Theorem)**.** *Let X be a nuclear space. For any characteristic functional Φ defined on X there exists a unique probability measure μ defined on the measurable space $(X', \mathcal{B})$, where X' is the dual space of X equipped with the weak topology and $\mathcal{B}$ is the Borel σ-algebra generated by the weak topology on X' such that*

$$\int_{X'} e^{i\langle \omega, \xi \rangle} d\mu(\omega) = \Phi(\xi), \quad \xi \in X.$$

Proposition C.0.4 (Proposition 1.2 [32])**.** *Let F be a completely monotonic function defined on the positive real line. Then, there exists a unique characteristic functional Φ, defined on a real separable Hilbert space H, such that*

$$\Phi(\xi) = F(||\xi||^2), \quad \xi \in H.$$

Appendix D

ggBergomi Implied Volatilities

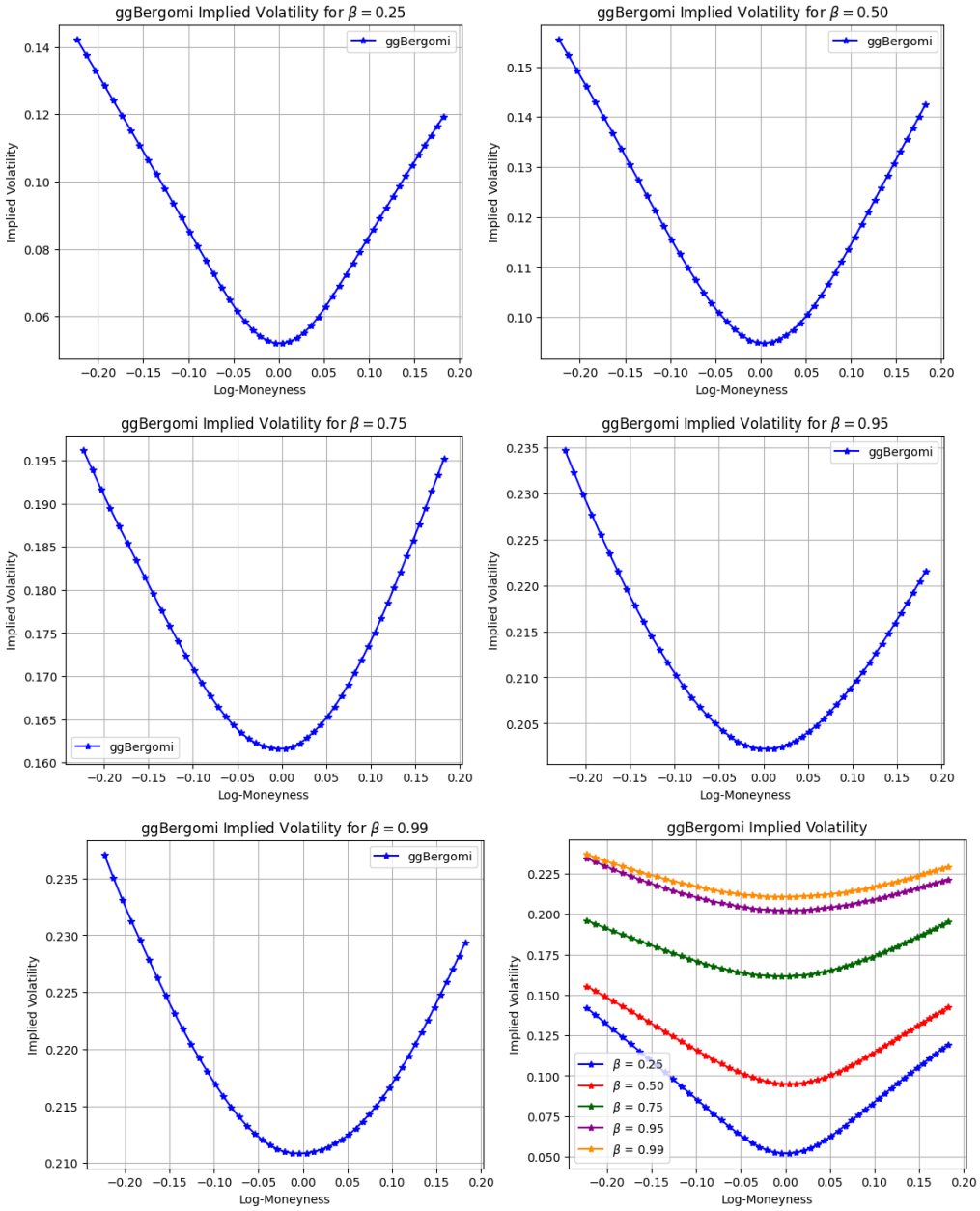

Figure D.1: Curve by Curve Implied Volatilities for $\beta \in \{0.25, 0.5, 0.75, 0.95, 0.99\}$.

Appendix E

The Hybrid Scheme

Definition E.0.1. Let W be a standard Brownian motion on a given filtered probability space $(\Omega, \mathcal{F}, (\mathcal{F}_t)_{t\geq 0}, \mathbb{P})$. A truncated Brownian semistationary ($\mathcal{BSS}$) process is defined as $\mathcal{B}(t) = \int_0^t g(t-s)\sigma(s)dW_s$, for $t \geq 0$, where σ is $(\mathcal{F}_t)_{t\geq 0}$-predictable with locally bounded trajectories and finite second, and $g : (0,\infty) \to [0,\infty)$ is Borel measurable and square integrable. We refer to it as a $\mathcal{BSS}(\tilde{\alpha}, W)$ process if, furthermore,

1. there exists $\tilde{\alpha}\backslash\{0\}$, where $\tilde{\alpha} := \frac{\alpha}{2} - \frac{1}{2}$, $\alpha \in (0,2)$, such that $g(x) = x^{\tilde{\alpha}} L_g(x)$ for all $x \in (0,1]$, where $L_g \in \mathcal{C}^1((0,1] \to [0,\infty))$, is slowly varying at the origin and bounded away from zero. Moreover, there exists a constant $C > 0$ such that $|L_g'(x)| \leq C(1 + x^{-1})$ for all $x \in (0,1]$;
2. the function g is differentiable on $(0,\infty)$.

Here the hybrid scheme in [6] is recalled. Following the notation in Definition E.0.1, we consider a (truncated) Brownian semistationary process $\mathcal{B}(\tilde{\alpha}, W)$, and introduce the truncation parameter $\kappa \in \mathbb{N}$. On an equidistant grid $\mathcal{T} := \{t_i = i/n\}_{i=0,\dots,n_T}$ with $n_T := \lfloor nT \rfloor$, for $n \geq 2$, the hybrid scheme for the $\mathcal{BSS}$ process $\mathcal{B}$ is approximated by $\mathcal{B}_n(t_i) = \widetilde{\mathcal{B}}_n(i) + \widehat{\mathcal{B}}_n(i)$ with

$$\widetilde{\mathcal{B}}_n(i) = \sum_{k=1}^{i\wedge\kappa} L_g\left(\frac{k}{n}\right)\sigma\left(\frac{i-k}{n}\right)\overline{W}_{i-k,k} \quad \text{and} \quad \widehat{\mathcal{B}}_n(i) = \sum_{k=\kappa+1}^{i} g\left(\frac{b_k^*}{n}\right)\sigma\left(\frac{i-k}{n}\right)\overline{W}_{i-k},$$

with L_g as in Definition E.0.1 and where

$$\overline{W}_i := \int_{t_i}^{t_{i+1}} dW_s,\ \overline{W}_{i,k} := \int_{t_i}^{t_{i+1}} (t_{i+k}-s)^{\tilde{\alpha}} dW_s,\ b_k^* = \left(\frac{k^{\tilde{\alpha}+1} - (k-1)^{\tilde{\alpha}+1}}{\tilde{\alpha}+1}\right)^{\frac{1}{\tilde{\alpha}}},\ \text{for } k \geq \kappa+1.$$

For any i, k, the random variables $\overline{W}_i$ and $\overline{W}_{i,k}$ are centered Gaussian with the following covariance structure:

$$\mathbb{E}[\overline{W}_{i,k}\overline{W}_i] = \frac{k^{\tilde{\alpha}+1} - (k-1)^{\tilde{\alpha}+1}}{n^{\tilde{\alpha}+1}\tilde{\alpha}+1}, \quad \text{and} \quad \mathbb{E}[\overline{W}_{i,k}\overline{W}_j] = 0,\ \text{for } k \neq j,$$

$$\mathbb{E}[\overline{W}_{i,k}\overline{W}_{i,j}] = \int_0^{\frac{1}{n}} \left(\frac{k}{n} - u\right)^{\tilde{\alpha}} \left(\frac{j}{n} - u\right)^{\tilde{\alpha}} du,\ \text{for } k \neq j,$$

$$\mathbb{V}[\overline{W}_{i,k}] = \frac{k^{2\tilde{\alpha}+1} - (k-1)^{2\tilde{\alpha}+1}}{n^{2\tilde{\alpha}+1}(2\tilde{\alpha}+1)},\ \mathbb{V}[\overline{W}_i] = \frac{1}{n}.$$

Bibliography

[1] M. Abramowitz and I. Stegun, *Handbook of mathematical functions*, Washington D.C., 1965.

[2] O. E. Barndorff-Nielsen and A. Veraart, *Stochastic volatility of volatility in continuous time*, CREATES research paper, 25 (2009).

[3] O. E. Barndorff-Nielsen and A. E. D. Veraart, *Stochastic Volatility of Volatility and Variance Risk Premia*, Journal of Financial Econometrics, 11 (2013), pp. 1–46.

[4] C. Bayer and S. Breneis, *Markovian approximations of stochastic Volterra equations with the fractional kernel*, 2022.

[5] C. Bayer, P. Friz, and J. Gatheral, *Pricing under rough volatility*, Quantitative Finance, 16 (2015), pp. 887–904.

[6] M. Bennedsen, A. Lunde, and M. S. Pakkanen, *Hybrid scheme for Brownian semistationary processes*, Finance and Stochastics, 21 (2017), p. 931–965.

[7] W. Bock, S. Desmettre, and J. L. da Silva, *Integral representation of generalized grey Brownian motion*, Stochastics, 92 (2020), pp. 552–565.

[8] O. Bonesini, A. Jacquier, and C. Lacombe, *A theoretical analysis of Guyon's toy volatility model*, 2022.

[9] F. Bourgey, S. D. Marco, and J. Delemotte, *Smile Dynamics and Rough Volatility*, July 2024. Available at SSRN: `https://ssrn.com/abstract=4911186`.

[10] D. Cahoy, *MWright: Mainardi-Wright Family of Distributions*, 2019-08-08. Version 0.3.2.

[11] D. O. Cahoy, *Estimation and simulation for the m-wright function*, Communications in Statistics - Theory and Methods, 41 (2012), pp. 1466–1477.

[12] M. Caputo, *Distributed order differential equations modelling dielectric induction and diffusion*, Fractional Calculus and Applied Analysis, 4 (2001), pp. 421–442.

[13] P. Carmona, L. Coutin, and G. Montseny, *Approximation of Some Gaussian Processes*, Statistical Inference for Stochastic Processes, 3 (2000), pp. 161–171.

[14] J. L. da Silva and M. Erraoui, *Singularity of generalized grey Brownian motions with different parameters*, Stochastic Analysis and Applications, 36 (2018), pp. 726–732.

[15] J. L. da Silva and M. Erraoui, *Singularity of generalized grey Brownian motion and time-changed Brownian motion*, in AIP Conference Proceedings, vol. 2286, AIP Publishing LLC, 2020, p. 020002.

[16] P. Doukhan, G. Oppenheim, and M. Taqqu, *Fractional Brownian motion and long-range dependence*, Birkhauser, Boston, 2002.

[17] D. Dufresne, *The Log-Normal Approximation in Financial and Other Computations*, Advances in Applied Probability, 36 (2004), pp. 747–773.

[18] O. E. Euch and M. Rosenbaum, *The characteristic function of rough Heston models*, 2016.

[19] W. Feller, *An Introduction to Probability Theory and its Applications*, Wiley, New York, 1966.

[20] J.-P. Fouque and Y. F. Saporito, *Heston stochastic vol-of-vol model for joint calibration of VIX and S&P 500 options*, Quantitative Finance, 18 (2018), pp. 1003–1016.

[21] P. K. Friz and J. Gatheral, *Computing the SSR*, 2024.

[22] R. Garra and R. Garrappa, *The Prabhakar or three parameter Mittag–Leffler function: Theory and application*, Communications in Nonlinear Science and Numerical Simulation, 56 (2018), pp. 314–329.

[23] P. Gassiat, *On the martingale property in the rough Bergomi model*, (2019).

[24] J. Gatheral, T. Jaisson, and M. Rosenbaum, *Volatility is rough*.

[25] J. Gatheral, P. Jusselin, and M. Rosenbaum, *The quadratic rough Heston model and the joint S&P 500/VIX smile calibration problem*, 2020.

[26] B. Horvath, A. Muguruza, and M. Tomas, *Deep Learning Volatility*, 2019.

[27] A. Jacquier, C. Martini, and A. Muguruza, *On VIX Futures in the rough Bergomi model*, 2017.

[28] A. Jacquier, Ž. Žurič, and A. Oliveri Orioles, *The Generalised Grey Bergomi Model*, 2024. unpublished.

[29] F. Mainardi, *Levy stable distributions in the theory of probability*, (2007).

[30] F. Mainardi, R. Gorenflo, and A. Vivoli, *Renewal processes of Mittag-Leffler and Wright type*, 2007.

[31] F. Mainardi, A. Mura, and G. Pagnini, *The Wright Function in Time-Fractional Diffusion Processes: A Tutorial Survey*, International Journal of Differential Equations, 2010 (2010), pp. 1–29.

[32] A. Mura and F. Mainardi, *A class of self-similar stochastic processes with stationary increments to model anomalous diffusion in physics*, 2007.

[33] A. Mura and G. Pagnini, *Characterizations and simulations of a class of stochastic processes to model anomalous diffusion*, Journal of Physics A: Mathematical and Theoretical, 41 (2008), p. 285003.

[34] A. Piryatinska, A. Saichev, and W. Woyczynski, *Models of anomalous diffusion: the subdiffusive case*, Physica A: Statistical Mechanics and its Applications, 349 (2005), pp. 375–420.

[35] I. Podlubny, *Fractional Differential Equations: An Introduction to Fractional Derivatives, Fractional Differential Equations, to Methods of their Solution and some of their Applications*, Academic Press, San Diego, 1999.

[36] L. C. G. Rogers, *Arbitrage with fractional Brownian motion*, Mathematical finance, 7 (1997), pp. 95–105.

[37] S. E. Rømer, *Empirical analysis of rough and classical stochastic volatility models to the SPX and VIX markets*, Quantitative Finance, 22 (2022), pp. 1805–1838.

[38] M. Rosenbaum and J. Zhang, *Deep calibration of the quadratic rough Heston model*, 2022.

[39] L. N. Trefethen, *Is Gauss quadrature better than Clenshaw–Curtis?*, SIAM Review, 50 (2008), pp. 67–87.

[40] Q. Zhu, G. Loeper, W. Chen, and N. Langrené, *Markovian Approximation of the Rough Bergomi Model for Monte Carlo Option Pricing*, Mathematics, 9 (2021), p. 528.